Central Nervous System Infection

Ashley H. Aiken

KEYWORDS

• CNS infections • Meningitis • Abscess • Encephalitis
• Subdural empyema

Infections of the brain and its linings pose a growing, worldwide health problem. Widespread immigration, the emergence of multidrug-resistant strains, and HIV infection have all served to change the face of the diagnosis and imaging of central nervous system (CNS) infections.

The radiologist plays a crucial role in identifying and narrowing the differential diagnosis of CNS infection. This article aims to outline a practical imaging approach, which begins with recognizing 1 of 5 basic imaging patterns: (1) extra-axial lesion, (2) ring-enhancing lesion, (3) temporal lobe lesion, (4) basal ganglia lesion, and (5) white matter abnormality.

Within these broad imaging categories, a thorough understanding of the characteristic imaging features of specific pathogens and clinical history, including patient immune status and geographic location, are essential to narrow the differential considerations and propose a more specific diagnosis.

Neuroimaging also plays a pivotal role in diagnosing and monitoring the therapeutic response in opportunistic infections in the setting of HIV. This subset of infections will also be discussed within the context of the 5 basic imaging patterns.

IMAGING MODALITIES

CT is often the first imaging study for the evaluation of suspected CNS infection because of its widespread availability and rapid assessment of complications such as hydrocephalus, mass effect/herniation, and hemorrhage. CT is critical in the emergency room setting to identify these neurosurgical emergencies. However, MRI is the study of choice for further characterization of CNS infection, and it is more sensitive for the identification of leptomeningitis, empyema, ventriculitis, and complications, such as cerebral infarction. The most important MR sequences in this setting include the following:

- Diffusion-weighted imaging (DWI)
- Fluid attenuated inversion recovery (FLAIR)
- T2-weighted (T2W)
- T1-weighted post-gadolinium (GAD)
- Magnetic resonance spectroscopy (MRS).

Diffusion-weighted imaging (DWI) plays an important role in differentiating a pyogenic abscess from other ring-enhancing lesions. Pyogenic abscesses classically have reduced diffusion ("light bulb bright diffusion"), which is thought to reflect the high viscosity of inflammatory cells. However, reduced diffusion is not specific to pyogenic abscess, and it may be present in other ring-enhancing lesions, including hypercellular tumor, subacute hematomas, and nonpyogenic infections.[1–9] DWI is also useful in detecting and characterizing extra-axial collections, as subdural empyemas typically have reduced diffusion.[7]

Fluid attenuated inversion recovery (FLAIR) imaging uses an inversion recovery pulse after an inversion time to nullify the high signal of cerebrospinal fluid (CSF). FLAIR is sensitive in detecting leptomeningeal disease because elevated protein in the subarachnoid space (SAS) causes a decrease in T1 relaxation time and resultant hyperintensity. In spite of the high sensitivity of FLAIR images in the detection of abnormal SAS

Division of Neuroradiology, Emory University Hospital, 1364 Clifton Road, Suite BG 26, Atlanta, GA 30322, USA
E-mail address: Ashley.aiken@emoryhealthcare.org

Neuroimag Clin N Am 20 (2010) 557–580
doi:10.1016/j.nic.2010.07.011
1052-5149/10/$ – see front matter

hyperintensity, this finding is not specific for leptomeningitis; it may also be encountered with leptomeningeal tumor, subarachnoid hemorrhage, supplemental O_2 administration, and severe arterial occlusive disease with slow flow in leptomeningeal collaterals.

T2-weighted (T2W) imaging is most helpful for evaluation the core signal intensity of ring-enhancing lesions, and to define the extent of surrounding vasogenic edema. T1-weighted post-gadolinium (GAD) imaging is critical to evaluate the enhancement characteristics of infectious etiologies. Specific patterns are discussed in the section on imaging patterns to follow.

Magnetic resonance spectroscopy (MRS) shows increases in lactate (1.3 ppm), acetate (1.92 ppm), and succinate (2.4 ppm) in pyogenic abscesses, presumably from the enhanced glycolysis and fermentation of the organism. Amino acids, including valine and leucine (0.9 ppm), are also known to be the end products of proteolysis by enzymes released by neutrophils in pus. Detection of resonance peaks from acetate, succinate, and such amino acids as valine and leucine is suggestive of abscess, as they have not been reported in proton MR spectra of brain tumors.[10–12]

IMAGING PATTERNS

Extra-axial

With this imaging pattern, it is key to search the paranasal sinuses, middle ear, and mastoid air cells for a source. It is also very important to look for complications including brain abscess, dural sinus thrombosis, infarction, and hydrocephalus.

Epidural empyema

An epidural abscess and/or empyema most commonly extends from the paranasal sinuses, especially the frontal sinus. Extension may be via direct bony erosion or retrograde flow via valveless bridging veins. Other etiologies include recent surgery, trauma, and mastoiditis. This purulent collection localizes outside the dura, which protects the underlying brain parenchyma. Therefore, patients with an epidural empyema tend to have a more benign, insidious course than those with a subdural empyema. Patients often complain only of a fever and headache.

On imaging, epidural abscesses are lentiform in shape, tacked down at the sutures, but they can cross the midline, unlike subdural collections (**Fig. 1**). The MR signal characteristics include T1 hypointensity, which is brighter than pure CSF given its proteinaceous content and inflammatory debris, and T2 hyperintensity, approaching CSF intensity. On post-GAD images, there is profound enhancement of the inflamed dura, often more than seen in subdural empyemas. Another important imaging feature of epidural empyemas is the relatively normal appearance of the underlying brain parenchyma in contrast to subdural empyemas.[13] Empyemas classically have reduced diffusion. However, the DWI signal characteristics can be more complex in epidural as opposed to subdural empyemas. Because epidural empyemas tend to have a more prolonged course, portions of the lesion may become less viscous, allowing for mixed intensity on DWI.[7] Please refer to "Acute Neuro-Interventional Therapies," elsewhere in this issue, for additional imaging information.

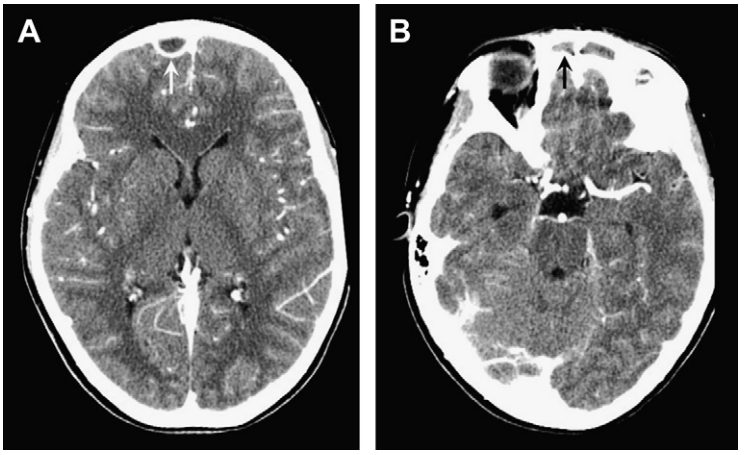

Fig. 1. Frontal sinusitis and epidural abscess. 11-year-old boy with severe headache. (*A*) Axial contrast-enhanced CT shows a right frontal peripherally enhancing lentiform collection (*arrow*), compatible with epidural abscess. (*B*) An inferior axial CT slice shows contiguous bilateral frontal sinus opacification (*arrow*).

Key Imaging Features: Epidural Empyema

- Lentiform collection
- Reduced diffusion
- Look for source in paranasal sinuses or mastoid air cells.

Subdural empyema

The source of most subdural empyemas is also sinusitis or mastoiditis, with frontal sinusitis accounting for most cases. Other etiologies include prior trauma with a superinfected subdural hematoma, postcraniotomy, or a complication of meningitis. Patients may present with fever, headache, seizures, and focal neurologic deficits. The subdural empyema is a medical emergency and usually requires neurosurgical intervention.

Neuroimaging plays a key role in early diagnosis and characterization. CT is often used acutely because of its speed and widespread availability. It is most useful in defining the extent and degree of mass effect and herniation; however, small subdural empyemas can be missed on CT, especially when located along the inner table of the skull.[14] MRI is helpful in diagnosing and differentiating a subdural empyema from other subdural collections, including a subdural effusion, chronic subdural hematoma, and a subdural hygroma that may mimic an empyema on CT (**Fig. 2**). Subdural empyemas have similar T1 and T2 signal characteristics to epidural empyemas, and classically show reduced diffusion, identified as high signal on DWI and low signal on the apparent diffusion coefficient (ADC) map.

Key Imaging Features: Subdural Empyema

- Reduced diffusion
- Look for source in paranasal sinuses or mastoid air cells

Leptomeningitis

Meningitis refers to acute or chronic inflammation of the pia-arachnoid layers and the adjacent CSF. It may be viral, bacterial, or fungal. The diagnosis usually is based on clinical history, physical examination, and CSF analysis, with imaging playing a limited role. The clinical presentation is often characteristic, with fever, headache, neck stiffness, vomiting, and photophobia being most common.

Imaging is most useful to evaluate the complications of meningitis, including vascular thrombosis, infarctions, brain abscess, ventriculitis, hydrocephalus, and extra-axial empyemas. Post-GAD and FLAIR sequences are most sensitive for detecting abnormal meningeal enhancement and SAS disease, respectively.[15] DWI is particularly helpful in the identification of complications, such as infarction or subdural empyema. Acute bacterial or viral meningitis typically shows enhancement over the cerebrum and interhemispheric fissure, whereas chronic tuberculous or fungal meningitis classically shows enhancement in the basal cisterns (**Fig. 3**).

Tuberculous meningitis, the most common presentation of neurotuberculosis, occurs predominately in young children and adolescents. It usually presents as a long-standing insidious process with exuberant inflammation of the basilar meninges and an obliterative vasculopathy of the basal penetrating vessels. Most infarcts are thus seen in the basal ganglia and internal capsule (see **Fig. 3**C).[16] The common imaging triad consists of basal meningeal enhancement, hydrocephalus, and cerebral infarction.[17] Leptomeningeal enhancement is not specific for infectious meningitis, and can also be seen with carcinomatous meningitis, sarcoidosis, or chemical meningitis.

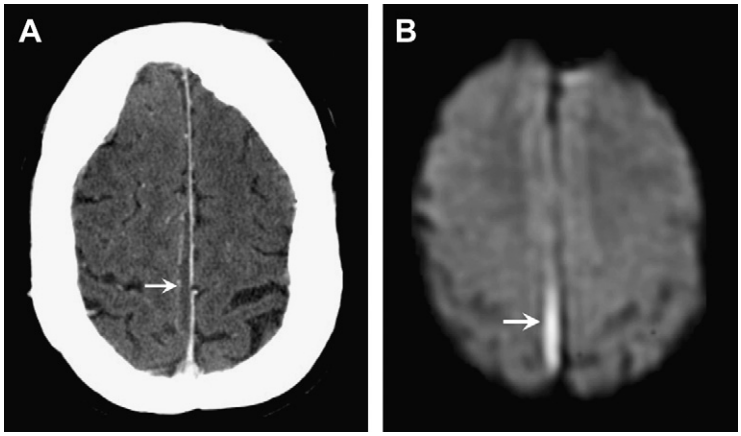

Fig. 2. Meningitis with subdural empyema. 56-year-old female with meningitis and new left leg shaking. (*A*) Axial contrast-enhanced CT shows a right parafalcine subdural collection (*arrow*). (*B*) DWI shows reduced diffusion compatible with subdural empyema (*arrow*).

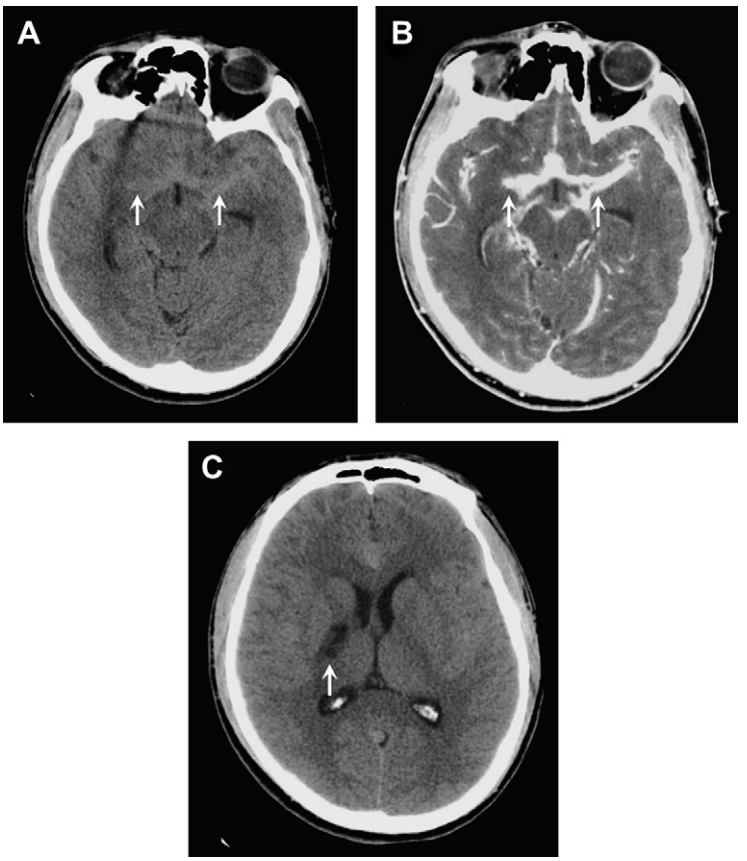

Fig. 3. **Coccidiomycosis and basilar meningitis.** 23-year-old migrant worker with headache and left upper extremity weakness. (*A*) Noncontrast CT shows hyperdensity in the basilar cisterns (*arrows*). (*B*) Contrast-enhanced CT shows abnormal enhancement of the basilar meninges (*arrows*). (*C*) Noncontrast CT at the level of the basal ganglia shows an infarct in the posterior limb of the right internal capsule (*arrow*), thus explaining the patient's clinical presentation. Perforating artery infarctions are a potential complication of basilar meningitis secondary to the associated inflammatory arteriopathy.

Key Imaging Features: Leptomeningitis

- SAS hyperintensity on FLAIR
- Leptomeningeal enhancement
- Look for hydrocephalus and infarctions as complications.

Ring-enhancing Lesions

This imaging pattern is the classic mimicker, and there is a long list of differential considerations. Frequently, the primary differential can be narrowed to infection versus neoplasm; however, close attention to the imaging features is critical to recognize nonoperative ring-enhancing lesions such as tumefactive demyelination, subacute infarct, and subacute hematoma. The imaging characteristics that favor infection over neoplasm include a thin, smooth, ring-enhancement, "daughter cysts," a thinner ring of enhancement toward the ventricular surface, and, of course, the "light bulb bright DWI" of a pyogenic abscess.

Pyogenic abscess

Pyogenic abscesses can arise from hematogenous dissemination, direct inoculation (trauma or surgery), contiguous extension (paranasal sinus, middle ear, mastoids), or complicating meningitis. The evolution of a pyogenic abscess progresses through 4 stages over approximately 2 weeks: (1) early cerebritis, (2) late cerebritis, (3) early abscess/capsule, and (4) late abscess/capsule. The MRI features of cerebritis and abscess depend on the stage of this infectious process.

In the early cerebritis stage, ill-defined T1 hypointensity and T2 hyperintensity are noted, with mottled heterogeneous enhancement. As the infection matures, the necrotic debris accumulates

centrally and the body attempts to isolate the infection with a collagenous capsule. Centrally, the abscess cavity is T1 hypointense (but slightly higher than CSF) and T2 hyperintense (Fig. 4). The abscess capsule is iso- or slightly hyperintense on T1-weighted images and markedly hypointense on T2-weighted imaging; this is thought to be secondary to paramagnetic hemoglobin degradation products or free radicals in macrophages. On post-GAD images, a thin, smooth ring is characteristic, in contrast to necrotic tumors, which typically have a thick nodular ring enhancement (Fig. 5). Another important feature of a brain abscess is its tendency to "grow toward the white matter," resulting in an oval configuration with a thicker enhancing capsule toward the more well-vascularized cortex. The thinner capsule abutting the white matter helps explain the propensity for intraventricular rupture and subsequent ventriculitis. Imaging features of ventriculitis/ependymitis include enhancement of the ventricular wall and reduced diffusion (Fig. 6). Ventriculitis is rarely isolated and usually occurs in the setting of abscess rupture, meningitis, or shunting and increases mortality to 80%.

DWI is extremely useful in identifying a brain abscess. As mentioned previously, the pyogenic brain abscess typically has "light bulb bright" diffusion signal intensity with corresponding low ADC values. Although some tumors can have low ADC values because of hypercellularity, the necrotic or cystic portions are usually less cellular and therefore do not show the same reduced diffusion.[1,2,4,6,9]

Key Imaging Features: Pyogenic Abscess

- "Light bulb bright" DWI
- Central T2 hyperintensity
- T2 hypointense capsule.

Tuberculoma

A global increase in the incidence of tuberculosis (TB) can be attributed to increased immigration, AIDS, and multidrug-resistant strains. CNS infection with *Mycobacterium tuberculosis* can present as either of the following:

- Diffuse form (eg, basal exudative leptomeningitis, as discussed previously)
- Localized form (eg, tuberculoma, abscess, or cerebritis).

The most common parenchymal form of CNS TB is tuberculous granuloma (tuberculoma). In some countries, TB represents up to 10% to 30% of all focal intracranial masses.

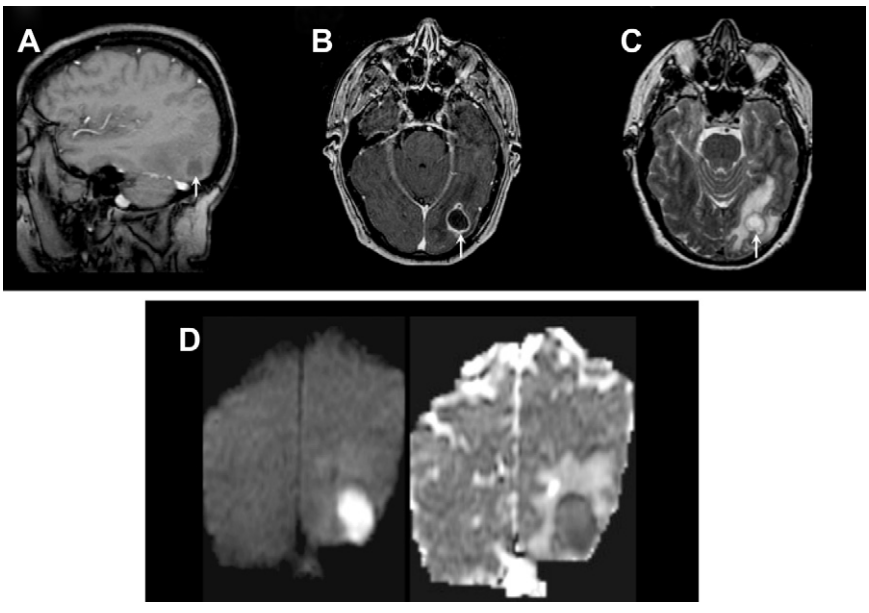

Fig. 4. **Pyogenic abscess.** 65-year-old woman with fever and vision loss. (*A*) Sagittal T1-weighted image shows the typical central T1 hypointensity (*arrow*). A T1 hyperintense rim can be seen in some cases. (*B*) Axial post-GAD T1-weighted image shows thin, smooth, ring enhancement that is typical for infection (*arrow*). Also, small daughter cysts are shown anteriorly and posteriorly. (*C*) Axial T2-weighted image shows the typical T2 hypointense rim, central T2 hyperintensity, and marked surrounding vasogenic edema, characteristic of the pyogenic brain abscess (*arrow*). (*D*) Axial DWI shows "light bulb" bright diffusion and hypointensity on the ADC map, consistent with true reduced diffusion.

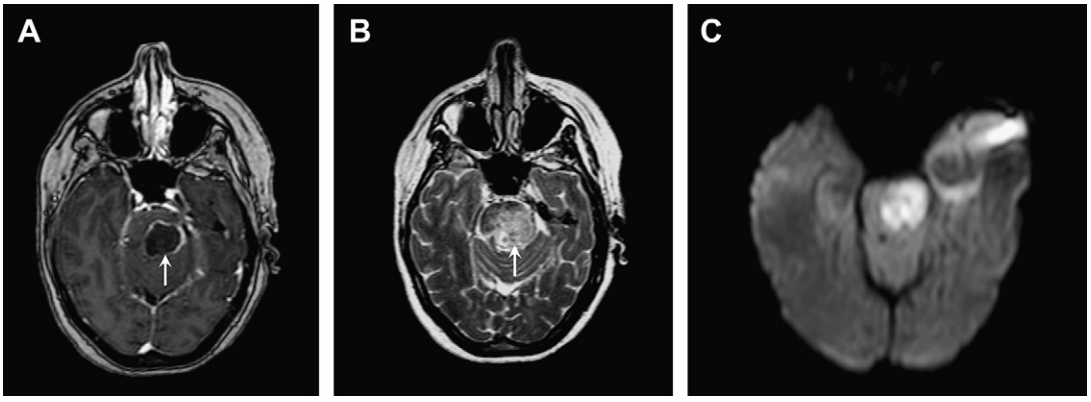

Fig. 5. Brainstem pyogenic abscess mimicking glioblastoma multiforme (GBM). 53-year-old man presented for preoperative evaluation for presumed GBM, without signs and symptoms of infection. (*A*) Axial post-GAD T1-weighted image shows thin, smooth enhancement of the pontine lesion (*arrow*), findings that are more suggestive of infection than neoplasm. (*B*) Axial T2-weighted image reveals ill-defined T2 hyperintensity (*arrow*) rather than the more typical discrete T2 hyperintensity; this finding suggests an earlier stage of infection. (*C*) Axial DWI and ADC map show reduced diffusion. Although GBMs may be hypercellular and show reduced diffusion, the combination of reduced diffusion and thin ring enhancement are key to the diagnosis of an abscess.

Parenchymal TB is more common in HIV-infected patients, can be solitary or multiple, and can occur with or without meningitis.[18] There is hematogenous spread in cases of known pulmonary TB.

Tuberculomas occur at the corticomedullary junction and are more common infratentorially in children and supratentorially in adults. The clinical presentation is often related to the space-occupying mass effect (ie, seizures, focal neurologic signs, headache, papilledema) rather than to the infection.

The MRI features depend on whether the granuloma is noncaseating, solid-caseating, or cystic-caseating. Noncaseating granulomas are T2 hypointense and solidly enhancing. Caseating granulomas have smooth ring enhancement. Solid caseating granulomas have characteristic T2 hypointensity (**Fig. 7**), whereas cystic-caseating granulomas have central T2 hyperintensity similar to pyogenic abscess. The dark T2 signal is thought to be caused by free radicals, and the solid caseation signal is attributed to cellular density.[17,19] Finally, the tuberculous abscess is a rare complication developing from parenchymal granulomas that are teeming with tubercle bacilli. Similar to cystic-caseating granulomas, these lesions show central T2 hyperintensity and even reduced diffusion, which can therefore mimic pyogenic abscess.[17,20] Some investigators suggest that MRS may help differentiate tubercular abscess from pyogenic abscess. Specifically, identification of the amino acids acetate and succinate are found in pyogenic abscesses, but lipid peaks are found in tubercular abscesses.[20]

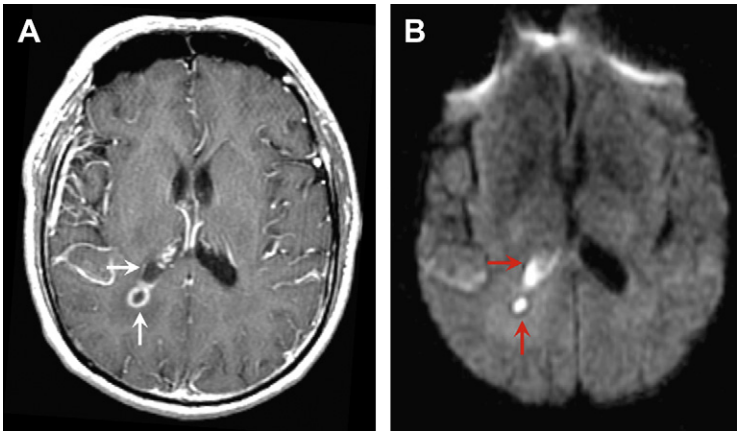

Fig. 6. Ventriculitis. 65-year-old man with fever after shunt placement. (*A*) Axial post-GAD T1-weighted image shows a ring-enhancing abscess adjacent to the atrium of the right lateral ventricle (*vertical arrow*). Note also subtle subependymal enhancement and higher signal intensity in the ventricle indicating ventriculitis (*horizontal arrow*). (*B*) Axial DWI at the same level demonstrates *reduced diffusion* in both the abscess (*vertical arrow*) and the debris within the ventricle (*horizontal arrow*).

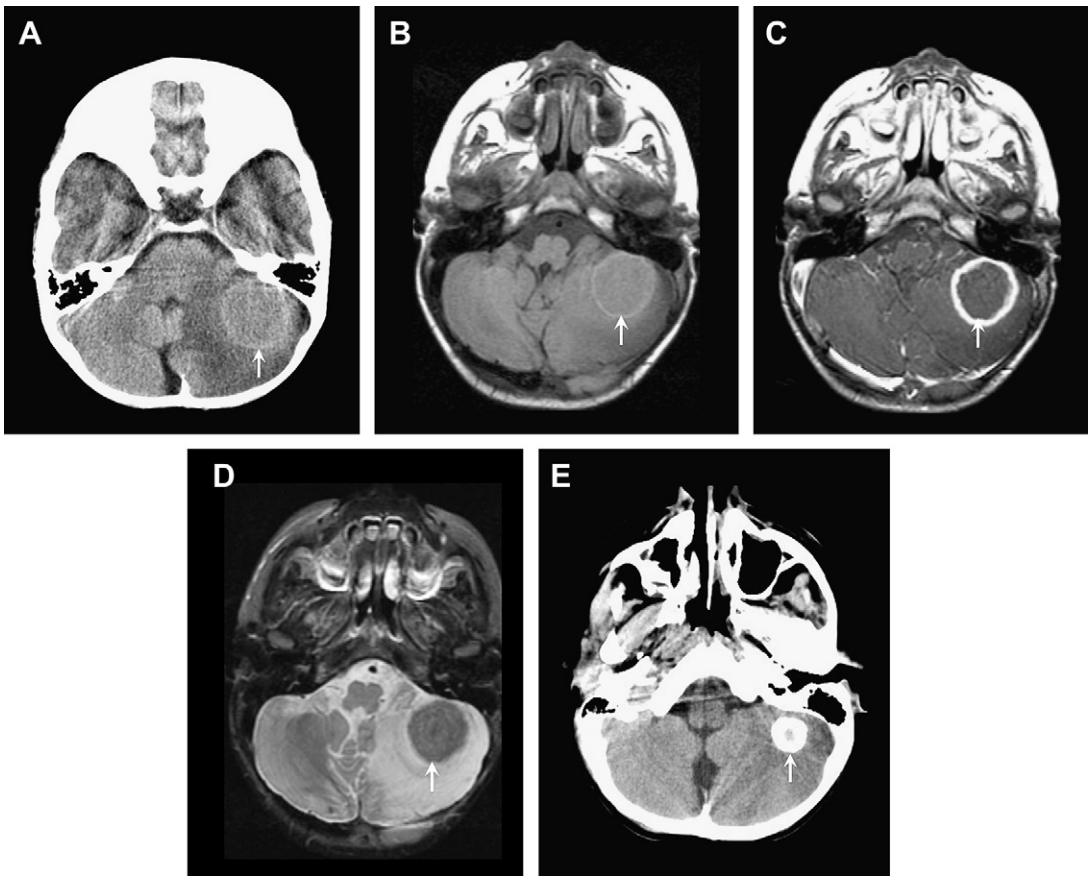

Fig. 7. **Caseating tuberculoma.** 3-year-old boy with fever, lethargy, and abnormal chest x-ray. (*A*) Axial noncontrast CT shows a round, slightly hyperdense mass with surrounding vasogenic edema located in the left cerebellar hemisphere (*arrow*). Note that the slight hyperdensity would be atypical for pyogenic abscess. (*B*) Axial noncontrast T1-weighted image reveals a thin hyperintense rim around the mass (*arrow*). (*C*) Axial post-GAD T1-weighted image shows smooth ring-enhancement (*arrow*), which favors infection over neoplasm. (*D*) Axial T2-weighted image shows uniform T2 hypointensity (*arrow*), which suggests an atypical infection rather than pyogenic infection. (*E*) Axial CT image obtained 1 year after treatment demonstrates dense calcification that is sometimes termed a "brain stone" (*arrow*).

Key Imaging Feature: Tuberculoma

- Central T2 hypointensity in noncaseating and solid caseating tuberculomas, ± reduced diffusion.

Neurocysticercosis

Neurocysticercosis, caused by the pork tapeworm *Taenia solium,* is the most common parasitic infection of the CNS in immunocompetent individuals. Endemic in Latin America and parts of Asia, India, Africa, and Eastern Europe, it is the most common cause of seizures in young patients in developing countries with poor hygiene. Neurocysticercosis may involve the brain parenchyma, the subarachnoid space, and the ventricles. [21–23]

CT and MRI findings in parenchymal neurocysticercosis depend on the stage of development of the parasite. Four stages have been categorized[24,25]: (1) viable/vesicular, (2) colloidal, (3) nodular-granular, and (4) calcified.

In the first, vesicular, stage, small cysts follow CSF density on CT and CSF intensity on MRI, and show little to no enhancement or edema. Most of these lesions have a "cyst with a dot" appearance representing an eccentric scolex (**Fig. 8**).

Colloidal lesions develop ring enhancement and surrounding edema as the parasite degenerates and triggers the host immune response. MRI characteristics in the second colloidal phase include central T1 hypointensity, central T2 hyperintensity, ring-enhancement, and *increased* diffusion (**Fig. 9**).

During the nodular-granular phase, the cyst wall thickens, the cyst involutes, and the surrounding edema decreases.

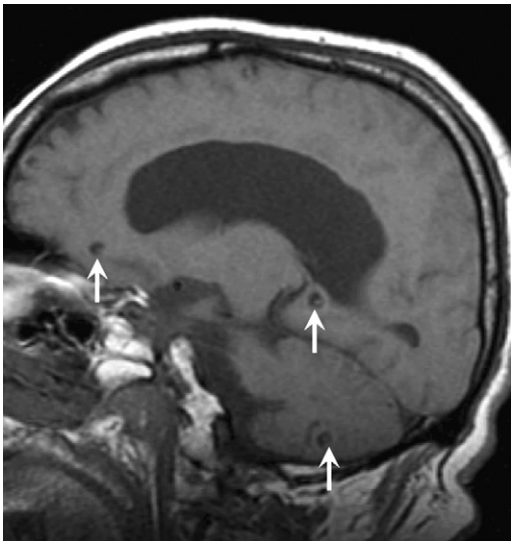

Fig. 8. **Vesicular stage of neurocysticercosis.** 40-year-old man with seizures. Sagittal T1-weighted image demonstrates multiple lesions that have a "cyst with a dot" appearance (*arrows*). This is a classic finding in vesicular neurocysticercosis where the "dot" represents the scolex. Note the *absence* of mass effect and edema.

Finally, the lesion mineralizes in the calcified stage and appears as small parenchymal calcifications on CT and small areas of susceptibility on MR gradient sequences (see **Fig. 9**D, E).

The colloidal stage mimics other ring-enhancing lesions. In these cases, DWI may be helpful to differentiate a cysticercosis cyst from a pyogenic abscess because cysticercal cysts are dark.[23] Also, ADC values are higher in neurocysticercosis than in TB granulomas.[26]

Subarachnoid lesions may be small in the cortical sulci, but are often large and "grapelike" when located in the basilar cisterns or Sylvian fissures. In the past, the term "racemose" referred to this form in which the scolex was not thought to develop; however, it is now known that the scolex may be present, yet undergoes degeneration, such that the term "racemose" has fallen into disuse.[23] Ruptured subarachnoid lesions may produce a basilar meningitis and lead to vasculitis and lacunar infarction.[23] Ventricular cysticerci are usually isodense to CSF on CT and isointense to CSF on T2-weighted MR imaging, thus making them difficult to detect. Intraventricular cysticercosis occurs in approximately 20% of cases and is most often located in the aqueduct of Sylvius or fourth ventricle.[13] Frequently, the accompanying hydrocephalus is detected before the obstructing cyst is identified. Therefore, FLAIR is a critical sequence to localize intraventricular cysts, because the cysts will appear hyperintense to CSF and become more conspicuous (**Fig. 10**). Cysts can migrate within the ventricular system (the "ventricular migration sign") and cause intermittent obstructive hydrocephalus.[27] Treatment includes antiparasitic medications such as oral albendazole, steroids for edema, and antiseizure medications in selected cases.[23]

Key Imaging Features: Neurocysticercosis

- Central T2 hyperintensity
- Dark DWI (*increased* diffusion)
- Scolex
- Additional calcifications.

Aspergillosis

Invasive CNS aspergillosis is rare, but is seen with increased frequency in immunosuppressed patients, particularly after bone marrow transplantation (BMT).[28] Because humans are infected by inhaling spores, the lungs and paranasal sinuses are the main sites of infection. Cerebral involvement may also result from hematogenous spread from the lungs or direct invasion from the sinuses. Invasive CNS aspergillosis has high morbidity and mortality, but case reports do note survival with early, aggressive antifungal therapy and surgical resection.[29,30] As clinical and laboratory features do not always confirm the diagnosis, neuroimaging plays a key role.[31]

Imaging patterns depend on lesion age and immunologic status of the patient. The angioinvasive nature of the fungus helps explain the CT and MR imaging features of these cortical and subcortical septic infarctions. Aspergillosis also has a unique affinity for perforating arteries that supply the basal ganglia, thalami, and corpus callosum.[32] In severely immunocompromised patients, the lesions appear as poorly defined areas of CT hypodensity or T2 hyperintensity on MRI, without significant mass effect, surrounding edema, or enhancement owing to the lack of a host immune response. In more immunocompetent patients, or as the immune function recovers after BMT, subtle peripheral or ring enhancement may be seen with surrounding vasogenic edema (**Fig. 11**).[28] Another important clue to the diagnosis is the presence of hemorrhage within these septic infarcts (seen as T1 hyperintensity, T2 hypointensity, and abnormal magnetic susceptibility on gradient sequences). In addition, pyogenic abscesses typically have a *smooth* outer wall, whereas fungal abscesses tend to have a *crenated* wall with intracavitary projections.[20] Although early septic infarcts may show reduced diffusion, Luthra and colleagues[20] found reduced diffusion only in

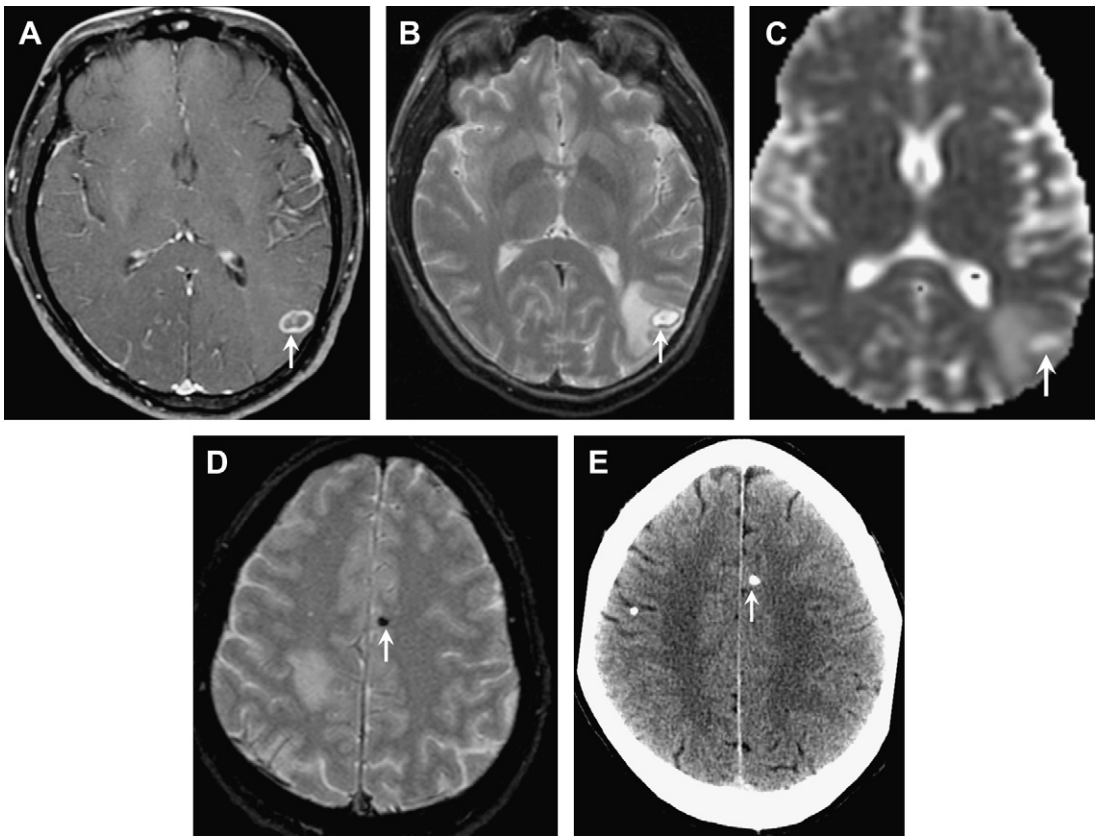

Fig. 9. Colloidal stage and nodular calcified stage of neurocysticercosis. 39-year-old man with new seizure. (*A*) Axial post-GAD T1-weighted image shows a ring-enhancing lesion (*arrow*) with a thin, smooth ring favoring infection. An eccentric, internal "dot" should always raise the possibility of neurocysticercosis. (*B*) Axial T2-weighted image also shows this eccentric "dot" (*arrow*). The central T2 hyperintensity and T2 hypointense rim can mimic pyogenic infection, but DWI should help distinguish. (*C*) Axial ADC map demonstrates *increased* rather than reduced diffusion (*arrow*), suggesting atypical infection rather than pyogenic infection. (*D*) Axial gradient-echo image demonstrates a focus of susceptibility (*arrow*). (*E*) Axial CT shows that the abnormal focus of susceptibility corresponds to calcification (*arrow*). Note the lack of edema and mass effect. Such calcifications are an important clue to the diagnosis of neurocysticercosis which represents the late calcified stage that easily seen on CT.

the wall and projections of the fungal abscess, whereas the core did not show reduced diffusion, distinguishing it from pyogenic and tubercular abscesses.

Key Imaging Features: Aspergillosis

- Angioinvasion with hemorrhage (T2 hypointensity + susceptibility)
- Septic infarcts with minimal mass effect and minimal to no enhancement
- Ring C+ only as immune function recovers
- Mycotic aneurysms.

Toxoplasmosis

Toxoplasmosis is caused by the parasite *Toxoplasma gondii* and is the most common mass lesion in patients with AIDS. Fortunately, the number of cases has declined significantly within the past decade because of the advent of highly active antiretroviral therapy (HAART).[33,34] *T gondii* is an obligate intracellular protozoan that exists in 3 forms: oocysts, tachyzoites, and bradyzoites. Tachyzoites are the rapidly multiplying form and they convert to bradyzoites or tissue cysts when they localize to the CNS.[34] Toxoplasmosis is a ubiquitous organism with titers as high as 70% in the normal adult population. The primary form of transmission is ingestion of undercooked meat, but also blood transfusions, contaminated needles, and contact with cat feces can result in the infection.[35] HIV-infected patients become most susceptible to toxoplasmosis when their CD4 counts are less than 100 cells/μL. The most common presenting symptom is headache, but fever, altered mental status, and focal deficits are also seen.[36]

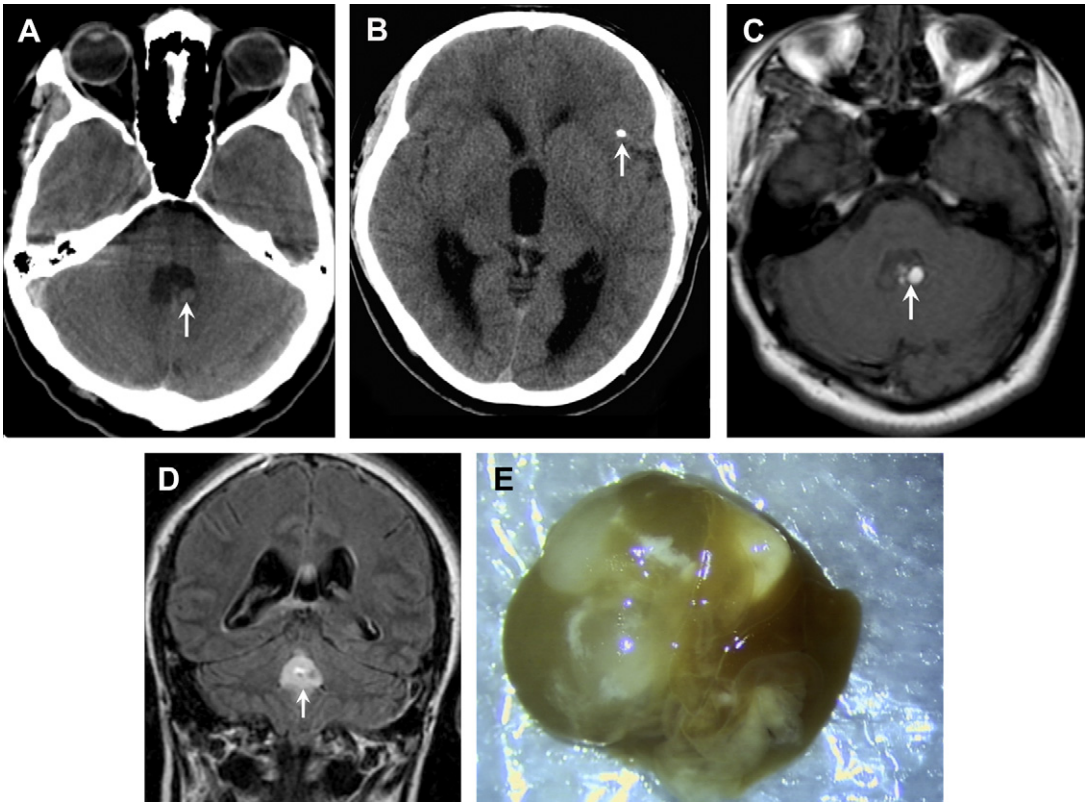

Fig. 10. Intraventricular neurocysticercosis. 30-year-old man with increasing headache. (*A*) Axial noncontrast CT shows enlargement of the fourth ventricle and a round eccentric nodule within the fourth ventricle (*arrow*). Note that the nodule appears too small to obstruct the fourth ventricle. (*B*) Axial CT at a higher level reveals enlargement of the lateral and third ventricles compatible with hydrocephalus. A clue to the etiology of the fourth ventricular lesion is the focal calcification in the left inferior frontal lobe (*arrow*). (*C*) Axial noncontrast T1-weighted image shows an atypical appearance consisting of intrinsic T1 hyperintensity in a neurocysticercosis cyst, secondary to proteinaceous debris (*arrow*). (*D*) Coronal FLAIR image shows that the cyst actually fills the *entire* fourth ventricle (*arrow*), explaining the obstructive hydrocephalus. This case illustrates why FLAIR can be helpful for identifying intraventricular cysts, as they can be difficult to see on CT and on T2-weighted images because they often follow CSF density and intensity, respectively. (*E*) Gross pathologic specimen revealing the proteinaceous components of this cyst.

On noncontrast CT, lesions are usually multiple, hypodense, and located in the basal ganglia, thalami, and corticomedullary junction.[37] The lesions frequently calcify after treatment. On MRI, the T2 signal characteristics can be variable, ranging from T2 hyperintense to T2 iso- or even hypointense.[38] On T1-weighted images, the lesions are hypointense, but intrinsic T1 shortening has been described in a few cases, thought to represent hemorrhage.[39] Smooth, ring enhancement is typically seen on post-GAD images, but smaller lesions may have more nodular enhancement. An imaging finding highly suggestive of toxoplasmosis is the "asymmetric target sign," which consists of a small eccentric nodule of enhancement along the enhancing wall, thought to represent infolding of the cyst wall (**Fig. 12**).[35] This sign is specific, but not sensitive (seen in ~30% cases).[34] Recently, a similar target sign has been described on FLAIR and T2-weighted imaging that consists of 3 layers: T2 hypointense core alternating with an intermediate zone of T2 hyperintensity and a T2 hypointense rim.[40] Although DWI signal can be variable in toxoplasmosis, most investigators have found that most lesions have *increased* diffusion on DWI.[8,41]

In the HIV-infected patient, the major differential consideration for multiple ring-enhancing lesions is primary CNS lymphoma. Imaging features that favor lymphoma include subependymal spread, reduced diffusion owing to hypercellularity, and corpus callosum involvement. Most patients are treated empirically for toxoplasmosis with

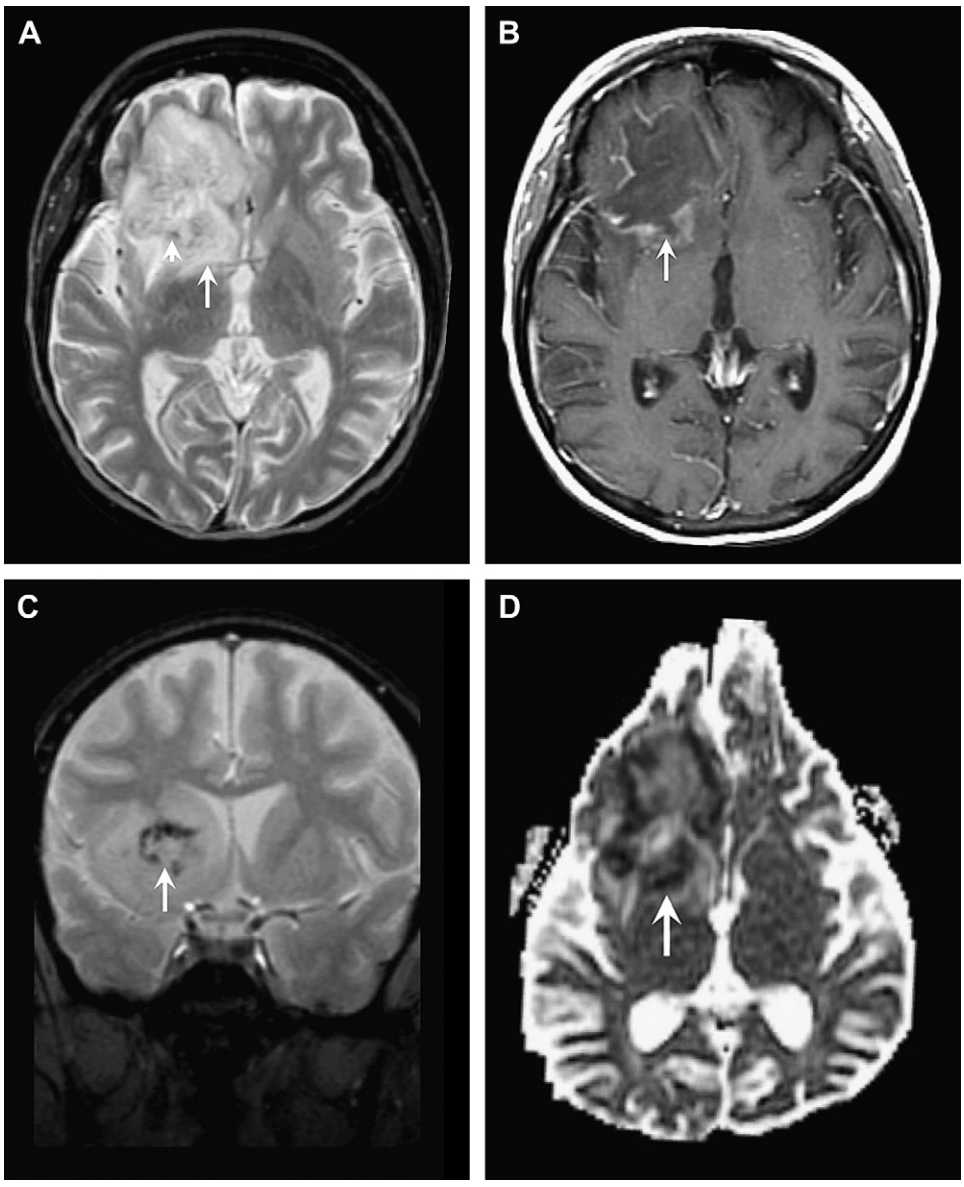

Fig. 11. Invasive aspergillosis. 11-year-old girl with neutropenia after bone marrow transplantation and new fevers. (*A*) Axial T2-weighted image shows a large, predominately T2 hyperintense lesion that involves most of the right inferior frontal lobe, putamen, and caudate head (*large arrow*). Note the small amount of mass effect given the size of the lesion. Also, note the small T2-hypointense areas within this lesion (*short arrow*). (*B*) Axial post-GAD T1-weighted image shows mild peripheral ring enhancement (*arrow*). Again, there is little to no mass effect. (*C*) Coronal gradient-echo image demonstrates susceptibility within this mass (*arrow*), consistent with hemorrhage. *Minimal enhancement, minimal mass effect, and hemorrhage are all clues* to diagnosis of invasive aspergillosis in this neutropenic patient. (*D*) Axial ADC map demonstrates reduced diffusion along the margins of the lesion (*arrow*), but no centrally reduced diffusion that is typical for pyogenic infection.

pyrimethamine and sulfadiazine for a duration of 6 weeks.[42] Radiographic improvement should occur in most (>90%) patients by 14 days.[36] If a follow-up MRI does not show improvement after empiric therapy, thallium-201 brain single-photon emission computed tomography (SPECT) or fluorodeoxyglucose positron emission tomography (FDG PET) may be useful. Both studies classically show increased uptake only in lymphoma, but have variable sensitivities. Other useful MR techniques include DWI, MRS, and MR perfusion. Lymphoma tends to have reduced diffusion because of its hypercellularity, whereas toxoplasmosis tends to show facilitated diffusion. MRS in

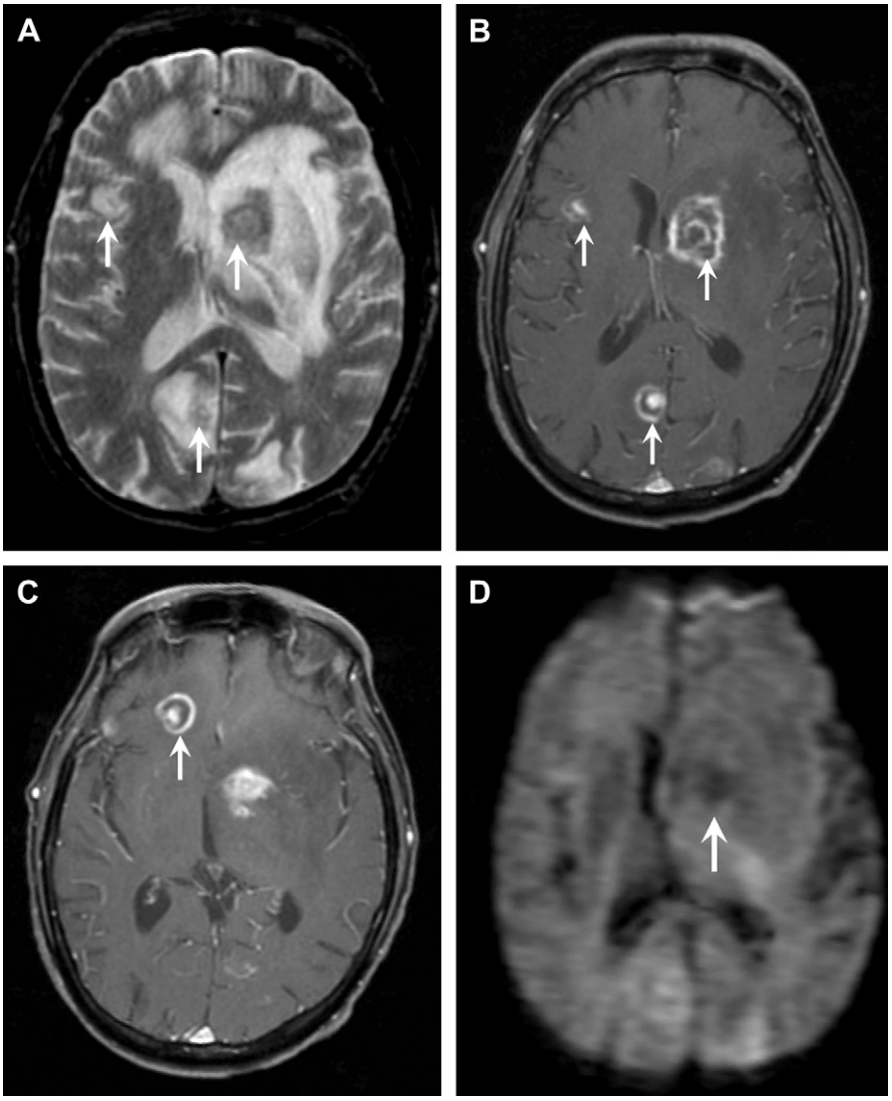

Fig. 12. Toxoplasmosis. 41-year-old HIV-positive man with new right-sided weakness. (*A*) Axial T2 image shows 3 dominant lesions with surrounding vasogenic edema: left caudate head, right parahippocampal gyrus, and right frontal lobe (*arrows*). Note that the 2 larger lesions are *T2 hypointense centrally*; this would be atypical for pyogenic abscess. (*B*) Axial T1-weighted post-GAD image shows ring enhancement (*arrows*). Note the "eccentric target sign," which is shown best in the right parahippocampal lesion. Although this sign is not sensitive, it is fairly specific for toxoplasmosis. (*C*) An additional axial T1-weighted post-GAD image shows another lesion in the right inferior frontal lobe, which also demonstrates the "eccentric target sign" (*arrow*). (*D*) Axial DWI shows no evidence of reduced diffusion within the left basal ganglia lesion (*arrow*).

lymphoma shows marked elevation of choline owing to hypercellularity and membrane turnover. In contrast, MRS in toxoplasmosis confirms the infectious origin with elevated lactate and lipid peaks. On MR perfusion, because lymphoma is a hypervascular neoplastic process, there is elevated relative cerebral blood volume (rCBV), whereas toxoplasmosis shows decreased rCBV.[43] In persistently equivocal cases, a biopsy is usually the next course of action.

Key Imaging Feature: Toxoplasmosis

- Asymmetric or eccentric target sign in the setting of an HIV patient with multiple ring-enhancing lesions.

Acute disseminated encephalomyelitis

Acute disseminated encephalomyelitis (ADEM) is a monophasic inflammatory demyelinating disorder associated with a recent infection or vaccination.[44] Infection or vaccination is thought

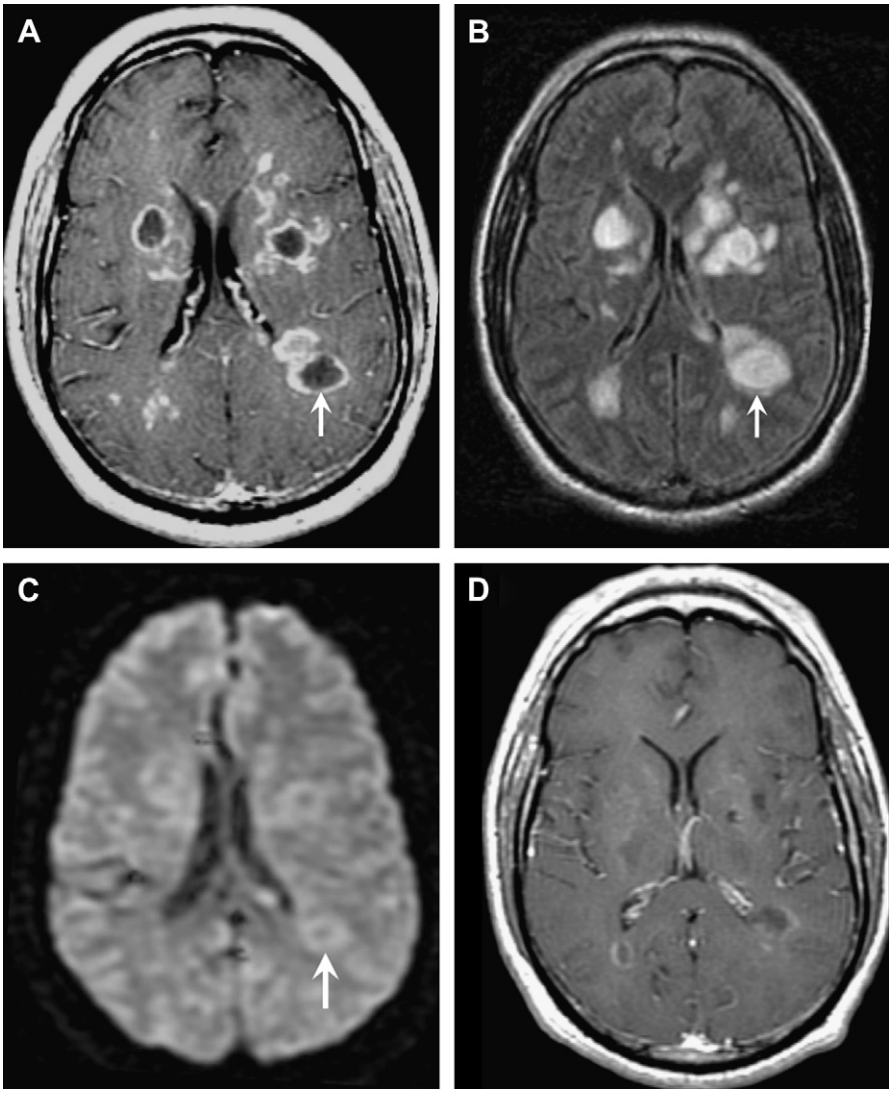

Fig. 13. Acute disseminated encephalomyelitis (ADEM). 43-year-old man with acute altered mental status. (*A*) Axial T1-weighted post-GAD image shows multiple ring-enhancing lesions along with additional smaller nodules of enhancement. (*B*) Axial FLAIR image shows T2 hyperintensity within these lesions; however, there is little to no surrounding vasogenic edema or mass effect. This is a clue that the lesion is a demyelinating process rather than tumor or infection. (*C*) Axial DWI shows no reduced diffusion, also mitigating against pyogenic infection. (*D*) Axial T1-weighted post-GAD image obtained 1 week following steroid treatment shows marked interval improvement with near resolution of many of the lesions.

to trigger an autoimmune attack, possibly via "molecular mimicry." Patients usually present with nonspecific symptoms, including headache, vomiting, fever, and lethargy. Children are affected more often than adults. On MR imaging, multifocal T2 hyperintense lesions are typically seen in the subcortical white matter, thalami, and basal ganglia, but lesions may be tumefactive and mimic other ring-enhancing infections and tumors (**Fig. 13**).[44,45] Therefore, it is crucial for the radiologist to consider tumefactive demyelination with all ring-enhancing lesions because of the drastically different management. Specifically, ADEM is treated medically with intravenous high-dose steroids and surgery should be avoided. Nonresponsive patients can also be treated with plasma exchange or immunoglobulins.

The imaging features most suggestive of tumefactive demyelinating lesions include large lesions with little to no mass effect, minimal edema, incomplete ring of enhancement at the "leading edge" of demyelination on the white

matter side of the lesion, central dilated veins within the lesion, and decreased perfusion (rCBV).[46–48]

Key Imaging Features: Acute Disseminated Encephalomyelitis

- Minimal mass effect
- Incomplete "leading edge" enhancement.

Temporal Lobe

When this imaging pattern is encountered, the primary diagnostic consideration should always be herpes encephalitis in the infectious category. Noninfectious considerations, including middle cerebral artery (MCA) infarct, glioma, and limbic encephalitis, are discussed briefly in the following sections.

Herpes encephalitis and other viral encephalitis

Encephalitis refers to a diffuse parenchymal inflammation seen as T2 hyperintensity on MR imaging. The most common viral encephalitides include herpes simplex viruses (HSV-1 and HSV-2), herpes zoster, arboviruses, and enteroviruses.[13]

HSV-1 is responsible for 95% of herpes encephalitides and occurs primarily in adults and older children. This devastating necrotizing encephalitis results from reactivation of latent HSV-1 infection within the trigeminal (or gasserian) ganglion, and is the most common cause of fatal sporadic encephalitis.[49] The infection spreads intracranially along meningeal branches of the trigeminal nerve, thus explaining the predilection for the temporal lobe. Patients typically present with fever, headaches, seizures, and focal neurologic deficits. The high mortality rate of HSV-1 herpes

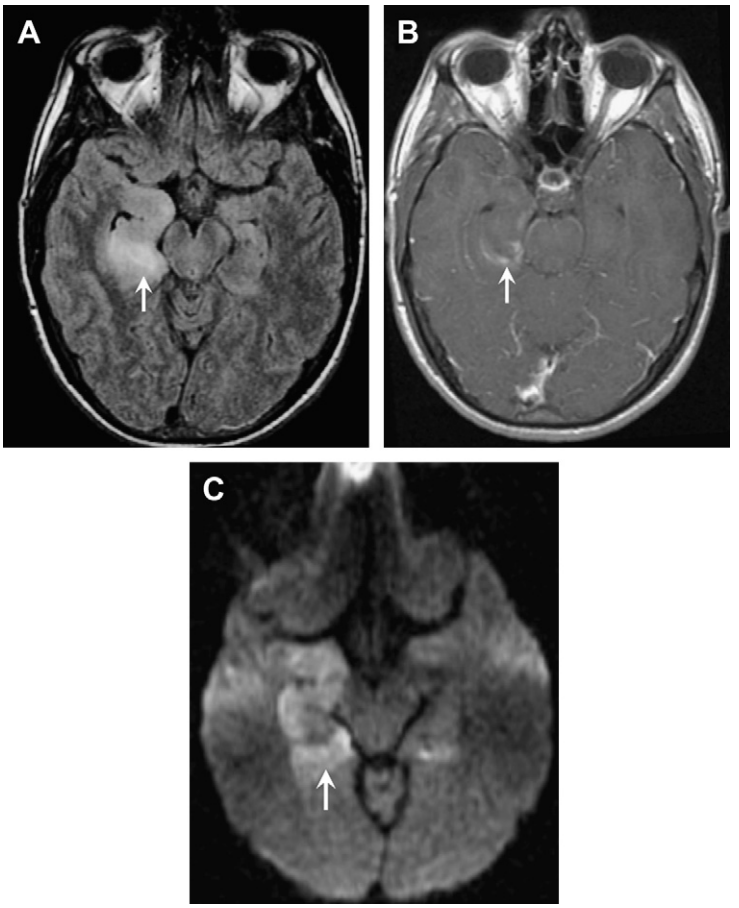

Fig. 14. **Herpes encephalitis.** 26-year-old man with new seizure and fever. (*A*) Axial FLAIR image demonstrates right medial temporal lobe enlargement and hyperintensity (*arrow*). (*B*) Axial T1-weighted post-GAD image shows slight linear enhancement posteriorly (*arrow*). Note that enhancement in HSV is variable and dependent on the time after onset. (*C*) Axial DWI shows reduced diffusion (*arrow*) and confirms involvement of the left medial temporal lobe.

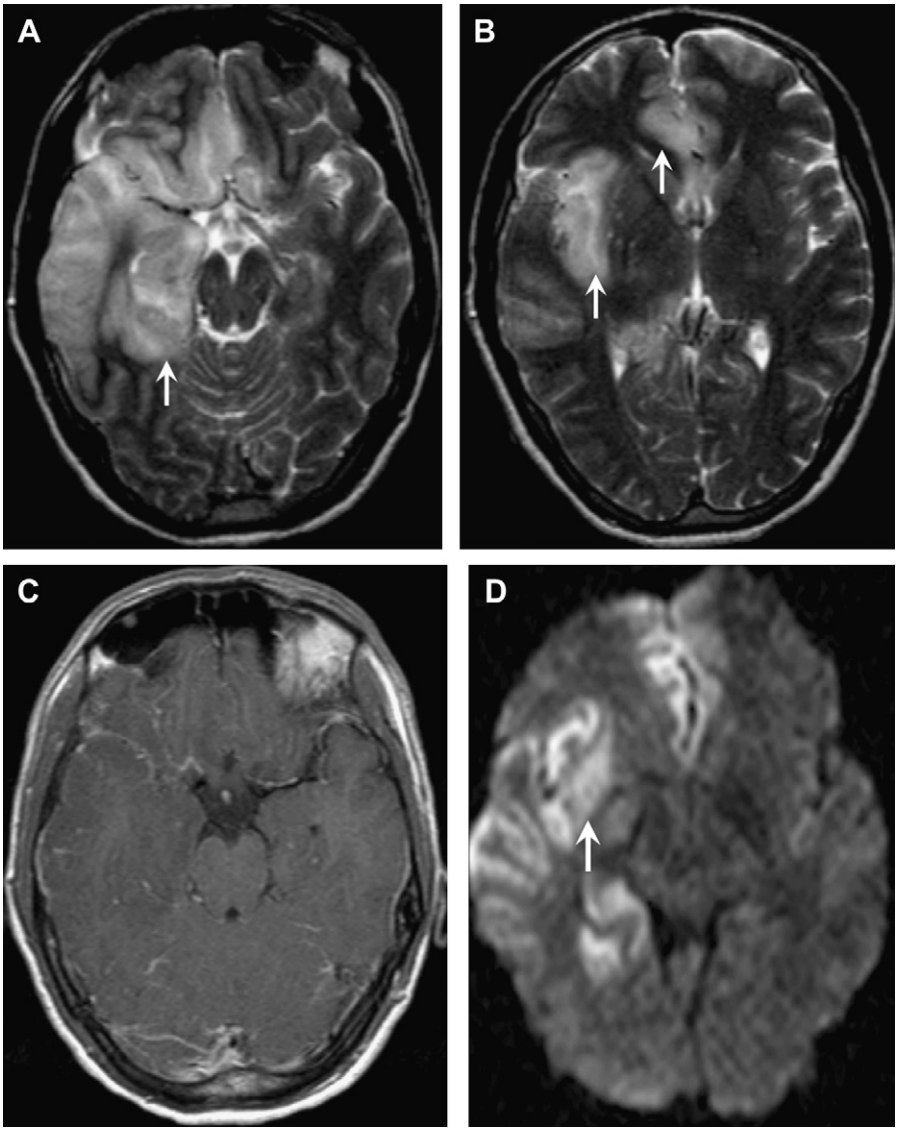

Fig. 15. **Herpes encephalitis (typical distribution).** 44-year-old woman with mental status changes. (*A, B*) Axial T2-weighted images at 2 different levels show bilateral, asymmetric involvement of the right temporal lobe, insula, and cingulate gyrus (*arrows*). (*C*) Axial T1-weighted post-GAD image shows little to no enhancement. (*D*) Axial DWI demonstrates reduced diffusion.

encephalitis, approaching 70% without treatment, and the availability of effective antiviral drugs, make early diagnosis key. Because polymerase chain reaction (PCR) is not 100% sensitive, early recognition of MR imaging findings can be critical.

The spectrum of imaging findings reflects the edema, hemorrhage, and necrosis seen pathologically. CT can be normal or show ill-defined areas of hypodensity in the medial temporal lobes and/or inferior frontal lobes. MRI better characterizes the extent of injury and classically shows bilateral, but asymmetric, involvement of the limbic system. Cortical swelling with T2 hyperintensity and T1 hypointensity are seen in the medial temporal lobe, insular cortex, cingulate gyrus, and inferior frontal lobe (**Figs. 14** and **15**). The pons may also be involved, likely from retrograde transmission along the cisternal segment of the trigeminal nerve.[49] Petechial hemorrhages can manifest as T1 shortening or abnormal susceptibility on gradient-echo sequences. T1 shortening can also be seen in a gyriform configuration owing to cortical hemorrhage.[50] Enhancement is variable, may be patchy or gyral, and generally develops later in the infection (after the T2 abnormality). Areas of reduced diffusion have been

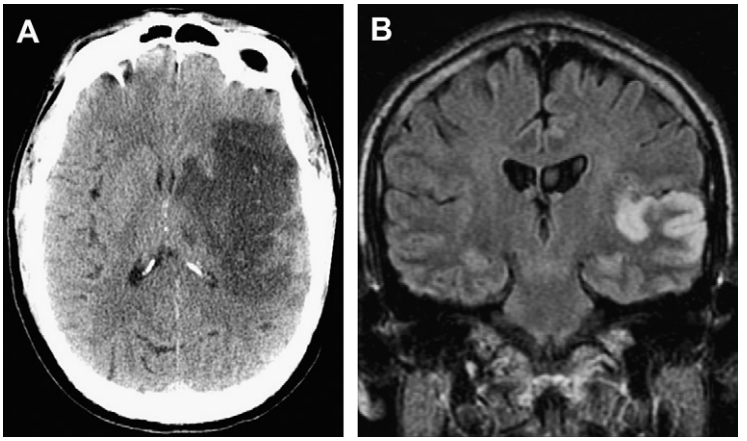

Fig. 16. **Middle cerebral artery infarction (contrast with HSV).** (*A*) Axial CT shows hypodensity involving the left basal ganglia and temporal lobe. Note that involvement of the basal ganglia is atypical for HSV and this distribution suggests a large left MCA infarct involving the M1 segment and lenticulostriate vessels. (*B*) Coronal FLAIR in a different patient shows hyperintensity in the lateral temporal lobe with relative sparing of the medial temporal lobe, suggesting MCA infarction rather than HSV. HSV usually involves the medial temporal lobe first.

shown to be one of the earliest findings[51,52]; however, DWI can be variable. Some investigators report more severe, nonresponsive cases to have reduced diffusion, whereas cases with a good response to treatment and more favorable outcome show resolution of reduced diffusion, or even increased diffusion at the onset.[53,54]

The primary differential considerations for abnormalities of the temporal lobe include MCA infarct, infiltrating gliomas, and limbic encephalitis. The basal ganglia are usually spared, and the medial temporal lobe is usually involved before the lateral temporal lobe, in herpes encephalitis, thus helping to differentiate from an acute MCA infarct (**Fig. 16**). The clinical history, including the onset and chronicity of symptoms, should help differentiate infarct from infiltrating tumor.

Key Imaging Feature: Herpes Encephalitis and Other Viral Encephalitis

- HSV-1 should be the diagnosis of choice in ANY patient with fever and signal abnormality in the medial temporal lobe until proven otherwise.

Basal Ganglia Lesions

Primary differential considerations for bilateral basal ganglia abnormalities include infection, toxic-metabolic etiologies, venous ischemia, hypoxic-ischemic injury, and neoplasm. It is critical to know the patient's history and specifically his or her immune status.

Cryptococcus

Cryptococcus neoformans is the most common CNS fungal infection in patients with AIDS and the third most common cause of CNS infection in AIDS, after HIV encephalopathy and toxoplasmosis.[34] It typically manifests as a chronic basilar meningitis or meningoencephalitis with minimal inflammation.[13] *C neoformans* is a ubiquitous yeastlike fungus found in soil contaminated by bird excreta. Patients are most vulnerable to *Cryptococcus* when their CD4 counts drop below 100 cells/μL. The diagnosis of CNS cryptococcosis can be made on the basis of a series of microbiologic investigations, including CSF culture and positive identification of the yeast with India ink staining; elevations in cryptococcal antigen latex agglutination titers in CSF and blood; and positive results with blood culture.

The most common imaging finding for cryptococcal meningitis, albeit nonspecific, is communicating or noncommunicating hydrocephalus.[55] Cryptococcus tends to spread along the perivascular (Virchow-Robin) spaces resulting in "gelatinous pseudocysts." These appear as multiple, nonenhancing, rounded, T2 hyperintense, T1 hypointense lesions in the basal ganglia (**Fig. 17**). Other imaging findings include meningeal enhancement and ring-enhancing granulomas ("cryptococcomas") with a predilection for the choroid plexus. Immunocompromised patients are less likely to have hydrocephalus or enhancing parenchymal lesions and are more likely to have gelatinous pseudocysts on imaging. Patients are treated with antifungal agents such as fluconazole or amphotericin B.

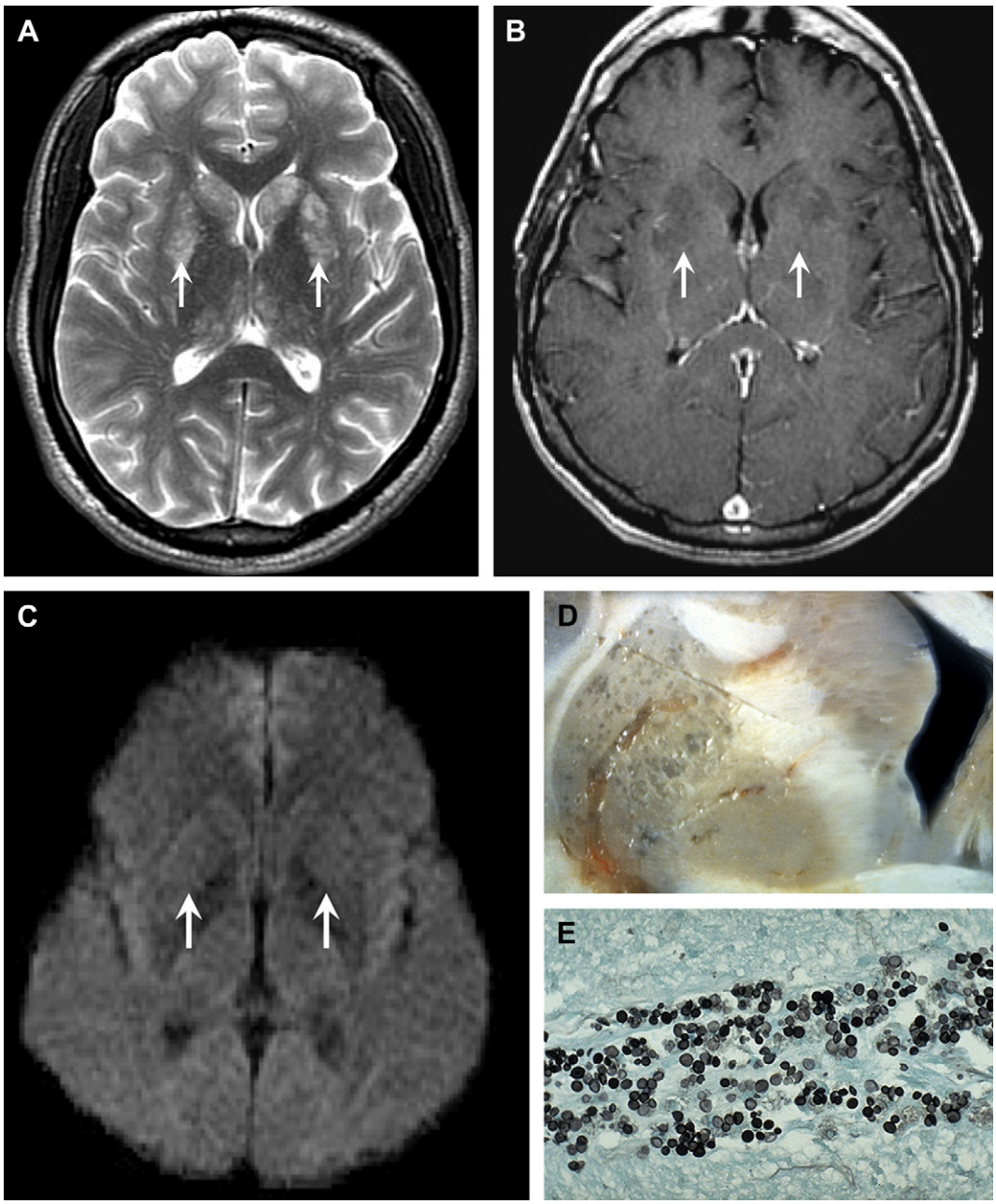

Fig. 17. Cryptococcal gelatinous pseudocysts. 47-year-old HIV-positive man with headache. (*A*) Axial T2-weighted image shows innumerable tiny T2 hyperintense foci within the caudate head, lentiform nuclei, and thalamus, bilaterally (*arrows*). (*B*) Axial T1-weighted post-GAD image shows *no enhancement*, thus excluding other entities found in the basal ganglia such as toxoplasmosis and lymphoma. (*C*) Axial DWI shows *no reduced diffusion*, thus excluding acute and/or subacute ischemic injury. (*D*) Coronal gross specimen at the level of the right frontal horn demonstrates mucinous material filling the putaminal perivascular spaces. (*E*) Histology slide shows positive India ink staining.

Key Imaging Features: Cryptococcus

- Nonenhancing T2 hyperintense lesions in the basal ganglia
- *Increased* diffusion.

Toxoplasmosis: Toxoplasmosis is a key differential consideration for ring-enhancing lesions in the basal ganglia in the HIV-infected patient. It was discussed previously in the section on ring-enhancing lesions.

Creutzfeldt-Jakob disease

Creutzfeldt-Jakob disease (CJD) is a rare fatal neurodegenerative disease characterized by rapidly progressive dementia. It is caused by an infectious protein known as a prion. Four different forms of CJD are known: the sporadic type (sCJD), the genetic type, the iatrogenic type, and the variant type (vCJD). The sporadic form is most common (85%).[56] Clinical diagnosis of probable sCJD includes at least 2 of 4 clinical features: myoclonus, visual or cerebellar disturbances, pyramidal/extrapyramidal dysfunction or akinetic mutism, and periodic sharp and slow wave complexes on EEG. The analysis of CSF for the 14-3-3 neuronal protein is also helpful.[56,57] The characteristic MR imaging features include "cortical ribboning" (ribbonlike hyperintensity in the gyri of the cerebral cortex on FLAIR and DWI), and hyperintensity of the caudate and putamen on FLAIR and DWI (**Fig. 18**). Variant CJD (vCJD) was first reported in the United Kingdom in 1996 and linked to bovine spongiform encephalopathy.[58] The classic imaging finding is the "pulvinar sign," seen as bright DWI and FLAIR signal in the pulvinar nucleus of the thalamus.

Key Imaging Features: CJD

- Bright DWI in putamen and caudate
- "Cortical ribboning"
- DWI is the most useful sequence to diagnose and follow these patients, especially because these patients are prone to motion degradation imaging.

White Matter Lesions

Lyme disease

Lyme disease is seen worldwide, but is the most common vector-borne disease in the United States. It is a tick-transmitted multisystem infection caused by the spirochete *Borrelia burgdorferi*. The incidence peaks in the summer months in the coastal northeast states, also Michigan and Minnesota.[59,60] The disease has 3 stages. Stage 1 occurs 3 to 32 days after the tick bite, with a characteristic targetlike rash, known as erythema migrans, and flulike symptoms. Stage 2 occurs after several weeks to months, consisting of neurologic (15% patients) and cardiac (8% patients) involvement.[59,61] Stage 3 can occur years later as chronic arthritis and neurologic symptoms. The diagnosis of Lyme disease should be based on a history of tick exposure, epidemiology, clinical signs and symptoms at different stages of the disease, and the use of serologic tests.

Lyme neuroborreliosis (LNB) may present with peripheral or central nervous system manifestations, including peripheral neuropathy, myelopathy, encephalitis, lymphocytic meningitis, and cranial nerve palsies. Involvement of the central nervous system is hypothesized to be either by retrograde spread via peripheral nerves or hematogenous spread, leading to a meningoencephalitis. Although the reported rate of abnormal MR findings in LNB varies from 17% to 43%, the most common imaging pattern is nonspecific abnormal white matter T2 prolongation, predominately in the frontal subcortical white matter (**Fig. 19**).[61–63] The distribution of brain involvement, including the callososeptal interface, may mimic a primary demyelinating disease such as multiple sclerosis (MS). When the characteristic clinical prodrome and exposure history are lacking, the multifocal clinical findings on neurologic examination, positive oligoclonal bands, and white matter patterns on MR imaging may confuse the diagnosis with MS. Patients may also present with leptomeningeal and cranial nerve enhancement, which is

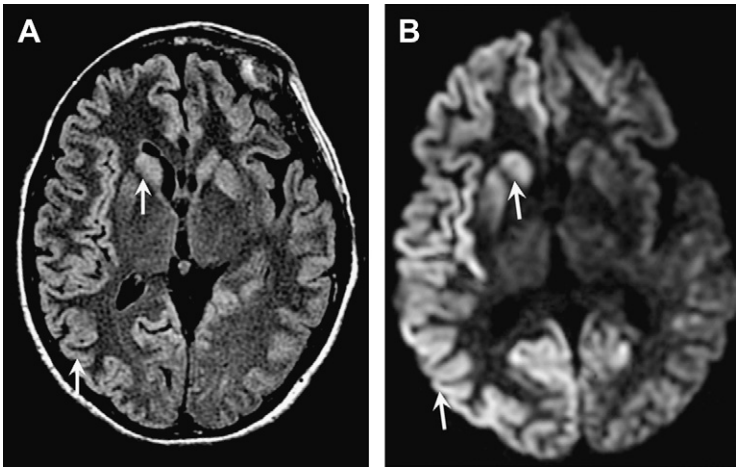

Fig. 18. Creutzfeldt Jacob disease. 60-year-old woman with rapidly progressive dementia. (*A*) Axial FLAIR image shows T2 hyperintensity in the caudate heads (*top arrow*) and putamina bilaterally. Note also abnormal hyperintensity of the cerebral cortex, greater on the right than left, consistent with so-called "cortical ribboning" (*bottom arrow*). (*B*) Axial DWI shows reduced diffusion in these same areas, predominately on the right.

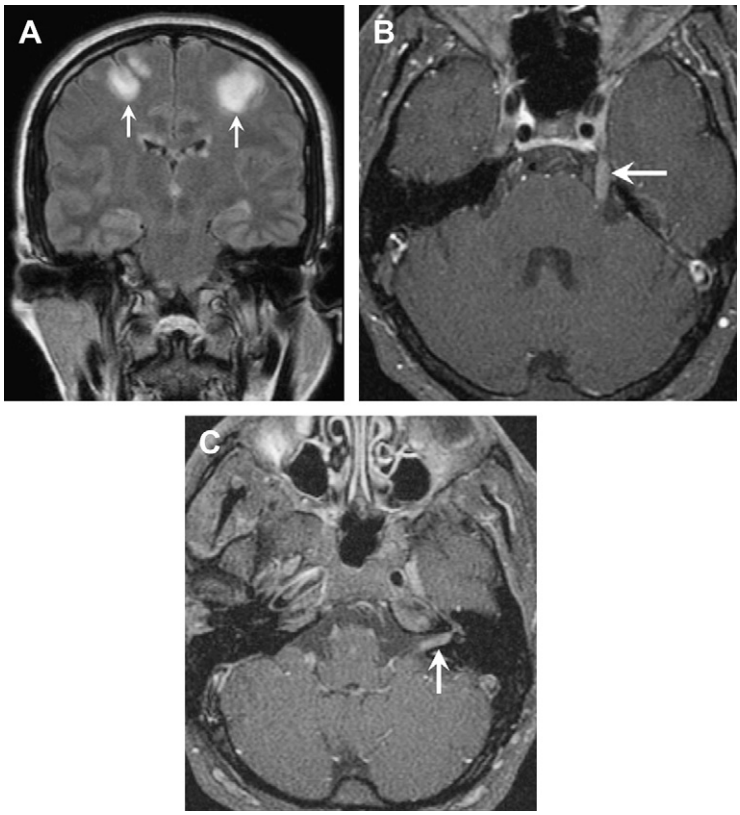

Fig. 19. Neuroborreliosis (Lyme disease). 19-year-old man with multiple cranial neuropathies. (*A*) Coronal FLAIR image shows bilateral T2 hyperintensity in the frontal white matter with extension to the cortex (*arrows*). No significant mass effect is noted. Lyme lesions can often mimic demyelinating disease. (*B, C*) Axial T1-weighted post-GAD images demonstrate enhancement of the left fifth, seventh, and eighth nerves (*arrows*).

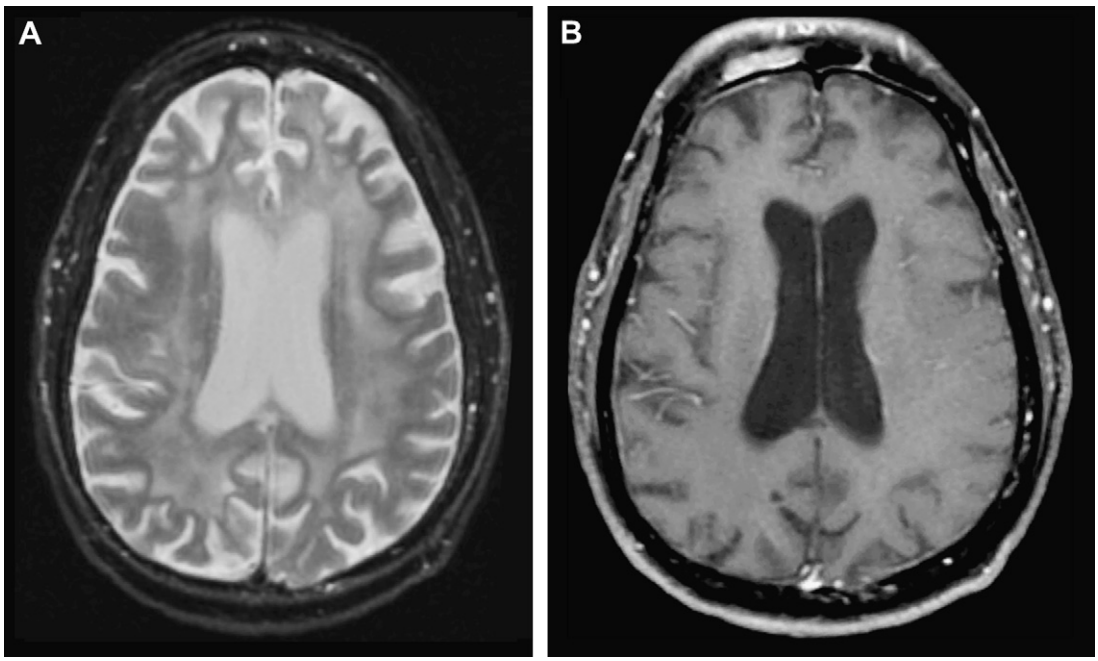

Fig. 20. HIV encephalopathy. 43-year-old HIV-positive man with dementia. (*A*) Axial T2-weighted image demonstrates global volume loss and diffuse periventricular white matter T2 hyperintensity. The history of HIV and the *symmetry* of the white matter abnormality are clues to the correct diagnosis of AIDS dementia complex. (*B*) Axial T1-weighted post-GAD image shows *no enhancement*. Note that the areas of T2 hyperintensity are barely visible on this T1-weighted image, ie, the lesions are T1 isointense.

not seen in MS, and is therefore another clue to the correct diagnosis in the setting of nonspecific white matter lesions (see **Fig. 19**B, C).[61]

Key Imaging Features: White Matter Lesions

- Multiple nonspecific T2 hyperintense lesions in the subcortical white matter
- Leptomeningeal and/or cranial nerve enhancement.

HIV encephalopathy

HIV encephalopathy is a progressive neurodegenerative disease resulting from direct infection of CNS mononuclear cells and microglial cells. Infected cells in the brain ultimately result in microglial activation, diffuse myelin loss, neuronal death, and astroglial proliferation.[64] Patients present with a subcortical dementia and cognitive and behavioral deficits including inattention,

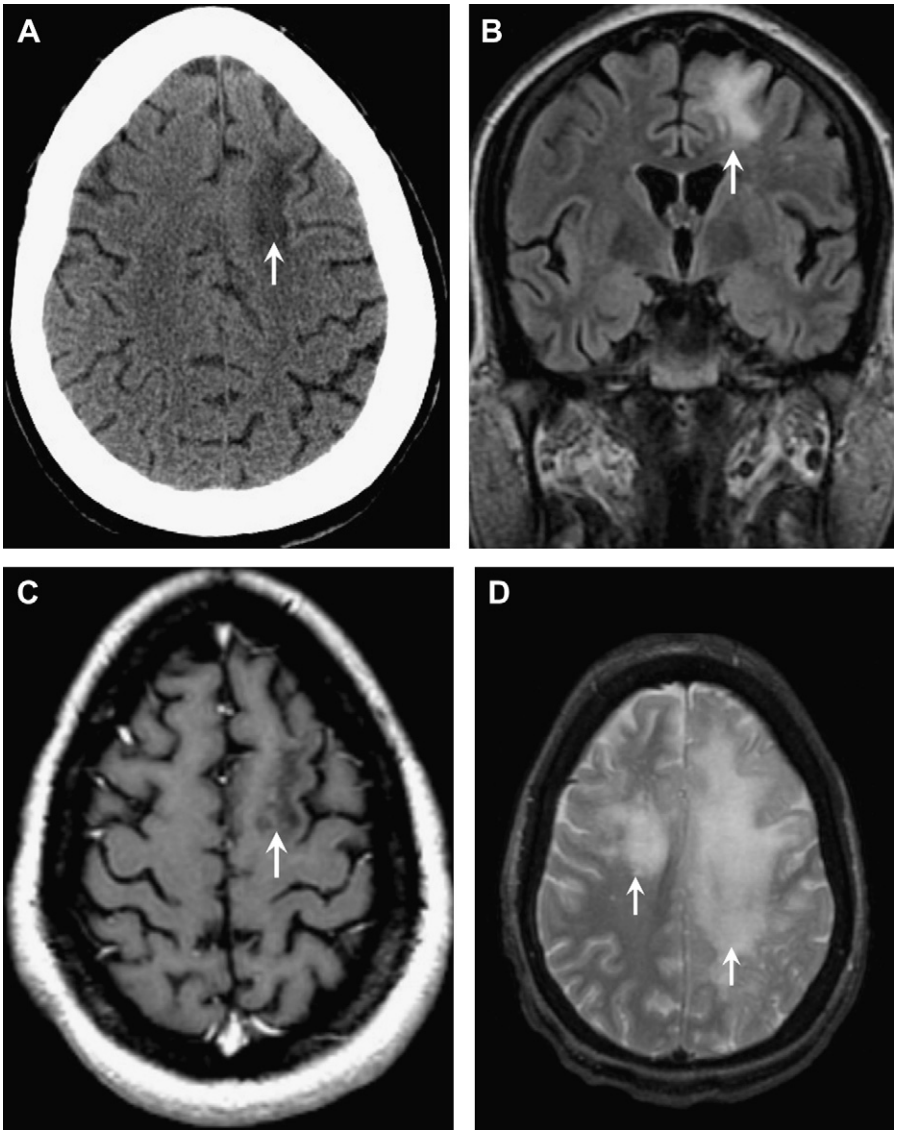

Fig. 21. Progressive multifocal leukoencephalopathy (PML). 34-year-old HIV-positive woman with right hand weakness. (*A*) Axial noncontrast CT image shows focal hypodensity within the subcortical white matter of the left superior frontal gyrus (*arrow*). (*B*) Coronal FLAIR image demonstrates corresponding T2 hyperintensity (*arrow*). Note *lack* of mass effect and involvement of subcortical U-fibers. (*C*) Axial T1-weighted post-GAD image shows no enhancement (*arrow*). Note the T1 hypointensity in contrast to the T1 isointense signal seen in the previous case of HIV encephalopathy (see **Fig. 20**B). (*D*) Three-month follow-up axial T2-weighted image in the same patient demonstrates rapid progression (*arrows*).

indifference and psychomotor slowing (AIDS Dementia Complex).

The imaging features of HIV encephalopathy include diffuse cerebral atrophy and *symmetric* T2 hyperintensity in the periventricular and deep white matter (**Fig. 20**). There is *no* mass effect or contrast enhancement. The symmetric white matter involvement helps to distinguish it from progressive multifocal leukoencephalopathy (PML), which tends to be asymmetric and involve subcortical U-fibers. HAART may not prevent HIV encephalopathy, but it can decrease the severity. Some studies have even shown that diffuse white matter abnormalities seen on brain MRI can exhibit partial resolution after HAART.[65]

Key Imaging Features: HIV Encephalopathy

- Diffuse cerebral atrophy
- Symmetric periventricular white matter T2 hyperintensity that is barely visible on T1-weighted images.

Progressive multifocal leukoencephalopathy

Progressive multifocal leukoencephalopathy (PML) is a progressive demyelinating disease caused by a DNA papovavirus, the John Cunningham virus (JC virus), which directly infects the myelin-producing oligodendrocytes. Although PML can be seen in many immunocompromised states, the greatest risk occurs in HIV-infected patients with CD4 counts ranging from 50 to 100 cells/μL. Other patients with impaired T-cell function, including patients with long-standing hematological disorders and immunosuppression after organ transplantation, are also at risk. Patients present with progressive neurologic decline. PCR testing of the CSF for the JC virus assists in making the diagnosis with approximately 96% specifivity.[34]

The typical MR imaging features include asymmetric T2 hyperintensity in the periventricular white matter with involvement of subcortical U-fibers that create a sharp border with the cortex (**Fig. 21**). Remarkably, the lesions are particularly hypointense on T1-weighted images. The involved areas may be single or multiple, unilateral or bilateral, but classically asymmetric with frequent involvement of the parieto-occipital areas. There is usually no enhancement or mass effect. These typical imaging features are seen in 90% of cases.[66] Atypical patterns can occur, however, including faint peripheral enhancement, mass effect, and even focal hemorrhage. Some investigators have described contrast enhancement as a positive development, heralding an inflammatory reaction and elimination of the JC virus, but it can also be seen with immune reconstitution syndrome exacerbating PML.[67] Reduced diffusion has been described in the early phases of the disease at the leading edge of active demyelination, and may be a poor prognostic sign indicating a phase of disease progression.[67–69]

The primary differential consideration is HIV encephalopathy, which can be distinguished from PML by its more symmetric white matter involvement, less intense T2 hyperintensity, lack of subcortical U-fiber involvement, and barely visible lesions on the T1-weighted sequence.

Key Imaging Features: Progressive Multifocal Encephalopathy

- Asymmetric white matter T2 hyperintensity
- Subcortical U-fibers involved
- T1 hypointense
- Typically no enhancement or mass effect.

PML and immune reconstitution inflammatory syndrome

Immune reconstitution following the initiation of combined antiretroviral therapy (HAART) may lead to activation of an inflammatory response to detectable or latent JC virus. Partial restoration of specific immunity may paradoxically lead to a worsening of a number of preexisting infections including PML, CMV, or *Cryptococcus*. Immune

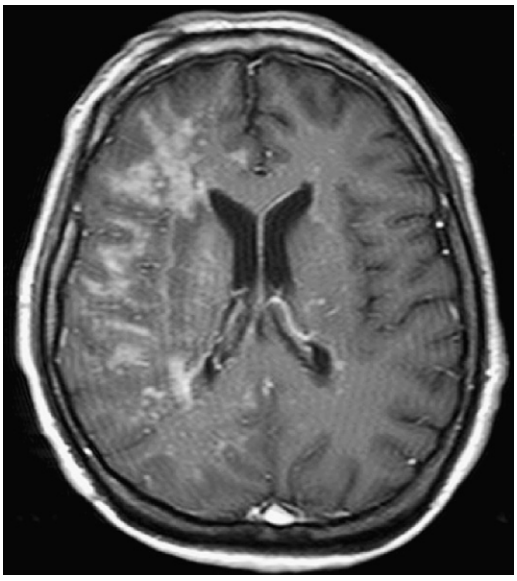

Fig. 22. Immune reconstitution syndrome (IRIS) in PML. 39-year-old HIV-positive man with acute worsening after initiation of HAART therapy. Axial T1-weighted post-GAD image shows extensive linear and nodular enhancement in this patient with PML. The enhancement is somewhat atypical for PML and should thus raise the possibility of lymphoma or immune reconstitution.

reconstitution inflammatory syndrome (IRIS) usually occurs in the initial months after beginning HAART, ranging from 1 week to 26 months in one study.[70] Patients with IRIS demonstrate paradoxic deterioration in their clinical status when their CD4 counts rise and viral replication appears to be under control. This often leads to a confusing clinical and radiographic picture. The neuroimaging features may vary depending on the underlying infection and timing of HAART therapy. Atypical imaging features may be encountered, such as mass effect and enhancement in PML lesions, which can mimic lymphoma (**Fig. 22**).

CMV encephalitis

CMV is a common herpes virus that does not cause clinical disease in immunocompetent patients, but can reactivate in the setting of immunosuppression. CMV infection usually occurs in patients with HIV when the CD4+ count falls less than 50 cells/μL. Although CNS involvement typically takes the form of a meningoencephalitis or ventriculitis, it can also present as myelitis, polyradiculitis, and retinitis. Therefore, CMV retinitis, which is seen in 25% of AIDS patients, may provide a clue to the diagnosis. Patients present with acute onset encephalitis and the diagnosis can be confirmed by positive CMVpp65 antigen.[71] CMV infection may progress to death within days. Patients are currently treated with gangcyclovir and foscarnet.

CMV involves the gray matter and ventricular ependyma to a greater degree than the white matter, thus distinguishing it from other encephalitides in patients with AIDS, such as HIV or PML.[13] Although imaging of CMV has low sensitivity and specificity, MRI is the method of choice. The most characteristic imaging finding is the presence of thin subependymal FLAIR hyperintensity and contrast enhancement (**Fig. 23**). CMV infection may also have a centrifugal spread from the ventricular system, with focal or diffuse increased T2 signal involving the gray matter or white matter.[13]

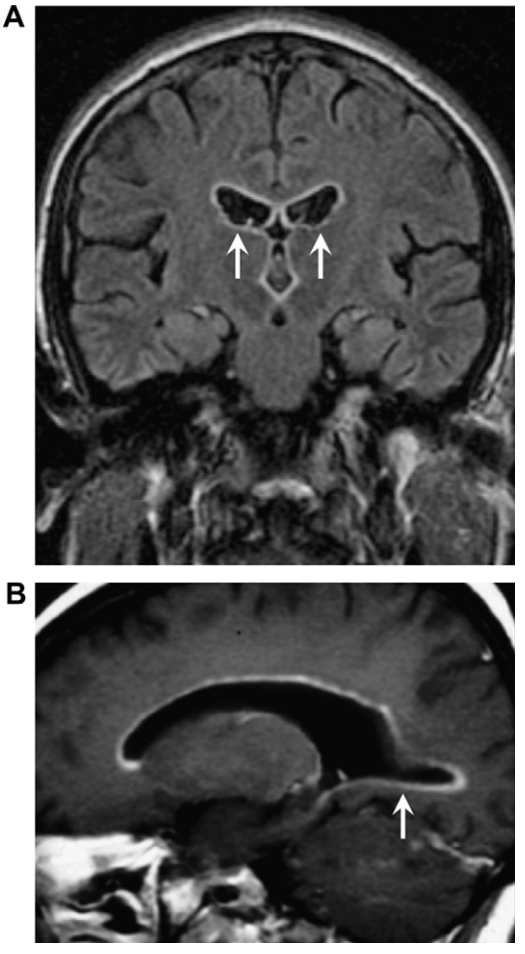

Fig. 23. Cytomegalovirus ventriculitis. 28-year-old HIV-positive woman with headache. (*A*) Coronal FLAIR image demonstrates a thin rim of T2 hyperintensity surrounding the frontal horns and third ventricle (*arrows*). (*B*) Parasagittal T1-weighted post-GAD image shows abnormal subependymal enhancement (*arrow*).

Key Imaging Feature: CMV Encephalitis

- Pencil-thin T2 hyperintensity surrounding the ventricles on FLAIR imaging with subependymal enhancement.

REFERENCES

1. Chiang IC, Hsieh TJ, Chiu ML, et al. Distinction between pyogenic brain abscess and necrotic brain tumour using 3-tesla MR spectroscopy, diffusion and perfusion imaging. Br J Radiol 2009;82(982): 813–20.
2. Desprechins B, Stadnik T, Koerts G, et al. Use of diffusion-weighted MR imaging in differential diagnosis between intracerebral necrotic tumors and cerebral abscesses. AJNR Am J Neuroradiol 1999; 20(7):1252–7.
3. Ferreira NP, Otta GM, do Amaral LL, et al. Imaging aspects of pyogenic infections of the central nervous system. Top Magn Reson Imaging 2005; 16(2):145–54.
4. Guo AC, Provenzale JM, Cruz LC Jr, et al. Cerebral abscesses: investigation using apparent diffusion coefficient maps. Neuroradiology 2001;43(5): 370–4.
5. Lai PH, Ho JT, Chen WL, et al. Brain abscess and necrotic brain tumor: discrimination with proton MR spectroscopy and diffusion-weighted imaging. AJNR Am J Neuroradiol 2002;23(8):1369–77.

6. Reddy JS, Mishra AM, Behari S, et al. The role of diffusion-weighted imaging in the differential diagnosis of intracranial cystic mass lesions: a report of 147 lesions. Surg Neurol 2006;66(3):246–50 [discussion: 250–1].
7. Tsuchiya K, Osawa A, Katase S, et al. Diffusion-weighted MRI of subdural and epidural empyemas. Neuroradiology 2003;45(4):220–3.
8. Camacho DL, Smith JK, Castillo M. Differentiation of toxoplasmosis and lymphoma in AIDS patients by using apparent diffusion coefficients. AJNR Am J Neuroradiol 2003;24(4):633–7.
9. Castillo M. Imaging brain abscesses with diffusion-weighted and other sequences. AJNR Am J Neuroradiol 1999;20(7):1193–4.
10. Burtscher IM, Holtas S. In vivo proton MR spectroscopy of untreated and treated brain abscesses. AJNR Am J Neuroradiol 1999;20(6):1049–53.
11. Chang KH, Song IC, Kim SH, et al. In vivo single-voxel proton MR spectroscopy in intracranial cystic masses. AJNR Am J Neuroradiol 1998;19(3):401–5.
12. Lai PH, Li KT, Hsu SS, et al. Pyogenic brain abscess: findings from in vivo 1.5-T and 11.7-T in vitro proton MR spectroscopy. AJNR Am J Neuroradiol 2005;26 (2):279–88.
13. Karampekios S, Hesselink J. Cerebral infections. Eur Radiol 2005;15(3):485–93.
14. Nathoo N, Nadvi SS, van Dellen JR, et al. Intracranial subdural empyemas in the era of computed tomography: a review of 699 cases. Neurosurgery 1999;44 (3):529–35 [discussion: 535–6].
15. Singer MB, Atlas SW, Drayer BP. Subarachnoid space disease: diagnosis with fluid-attenuated inversion-recovery MR imaging and comparison with gadolinium-enhanced spin-echo MR imaging—-blinded reader study. Radiology 1998;208(2):417–22.
16. Gupta RK, Gupta S, Singh D, et al. MR imaging and angiography in tuberculous meningitis. Neuroradiology 1994;36(2):87–92.
17. Bernaerts A, Vanhoenacker FM, Parizel PM, et al. Tuberculosis of the central nervous system: overview of neuroradiological findings. Eur Radiol 2003;13(8): 1876–90.
18. Garcia-Monco JC. Central nervous system tuberculosis. Neurol Clin 1999;17(4):737–59.
19. Jinkins JR, Gupta R, Chang KH, et al. MR imaging of central nervous system tuberculosis. Radiol Clin North Am 1995;33(4):771–86.
20. Luthra G, Parihar A, Nath K, et al. Comparative evaluation of fungal, tubercular, and pyogenic brain abscesses with conventional and diffusion MR imaging and proton MR spectroscopy. AJNR Am J Neuroradiol 2007;28(7):1332–8.
21. Del Brutto OH, Sotelo J. Neurocysticercosis: an update. Rev Infect Dis 1988;10(6):1075–87.
22. Garcia HH, Del Brutto OH. Imaging findings in neurocysticercosis. Acta Trop 2003;87(1):71–8.
23. Castillo M. Imaging of neurocysticercosis. Semin Roentgenol 2004;39(4):465–73.
24. Escobar A, Aruffo C, Cruz-Sanchez F, et al. [Neuropathologic findings in neurocysticercosis]. Arch Neurobiol (Madr) 1985;48(3):151–6 [in Spanish].
25. Carpio A, Placencia M, Santillan F, et al. A proposal for classification of neurocysticercosis. Can J Neurol Sci 1994;21(1):43–7.
26. Gupta RK, Prakash M, Mishra AM, et al. Role of diffusion weighted imaging in differentiation of intracranial tuberculoma and tuberculous abscess from cysticercus granulomas—a report of more than 100 lesions. Eur J Radiol 2005;55(3):384–92.
27. Rangel-Guerra RA, Herrera J, Elizondo G, et al. Neurocysticercosis. Arch Neurol 1988;45(5):492.
28. Guermazi A, Gluckman E, Tabti B, et al. Invasive central nervous system aspergillosis in bone marrow transplantation recipients: an overview. Eur Radiol 2003;13(2):377–88.
29. Schwartz S, Milatovic D, Thiel E. Successful treatment of cerebral aspergillosis with a novel triazole (voriconazole) in a patient with acute leukaemia. Br J Haematol 1997;97(3):663–5.
30. Khoury H, Adkins D, Miller G, et al. Resolution of invasive central nervous system aspergillosis in a transplant recipient. Bone Marrow Transplant 1997;20(2):179–80.
31. DeLone DR, Goldstein RA, Petermann G, et al. Disseminated aspergillosis involving the brain: distribution and imaging characteristics. AJNR Am J Neuroradiol 1999;20(9):1597–604.
32. Foerster BR, Thurnher MM, Malani PN, et al. Intracranial infections: clinical and imaging characteristics. Acta Radiol 2007;48(8):875–93.
33. Levy RM, Mills CM, Posin JP, et al. The efficacy and clinical impact of brain imaging in neurologically symptomatic AIDS patients: a prospective CT/MRI study. J Acquir Immune Defic Syndr 1990;3(5):461–71.
34. Smith AB, Smirniotopoulos JG, Rushing EJ. From the archives of the AFIP: central nervous system infections associated with human immunodeficiency virus infection: radiologic-pathologic correlation. Radiographics 2008;28(7):2033–58.
35. Ramsey RG, Geremia GK. CNS complications of AIDS: CT and MR findings. AJR Am J Roentgenol 1988;151(3):449–54.
36. Porter SB, Sande MA. Toxoplasmosis of the central nervous system in the acquired immunodeficiency syndrome. N Engl J Med 1992;327(23):1643–8.
37. Navia BA, Petito CK, Gold JW, et al. Cerebral toxoplasmosis complicating the acquired immune deficiency syndrome: clinical and neuropathological findings in 27 patients. Ann Neurol 1986;19(3):224–38.
38. Brightbill TC, Post MJ, Hensley GT, et al. MR of Toxoplasma encephalitis: signal characteristics on T2-weighted images and pathologic correlation. J Comput Assist Tomogr 1996;20(3):417–22.

39. Trenkwalder P, Trenkwalder C, Feiden W, et al. Toxoplasmosis with early intracerebral hemorrhage in a patient with the acquired immunodeficiency syndrome. Neurology 1992;42(2):436–8.
40. Masamed R, Meleis A, Lee EW, et al. Cerebral toxoplasmosis: case review and description of a new imaging sign. Clin Radiol 2009;64(5):560–3.
41. Batra A, Tripathi RP, Gorthi SP. Magnetic resonance evaluation of cerebral toxoplasmosis in patients with the acquired immunodeficiency syndrome. Acta Radiol 2004;45(2):212–21.
42. Nath A, Sinai AP. Cerebral toxoplasmosis. Curr Treat Options Neurol 2003;5(1):3–12.
43. Ernst TM, Chang L, Witt MD, et al. Cerebral toxoplasmosis and lymphoma in AIDS: perfusion MR imaging experience in 13 patients. Radiology 1998;208(3):663–9.
44. Menge T, Hemmer B, Nessler S, et al. Acute disseminated encephalomyelitis: an update. Arch Neurol 2005;62(11):1673–80.
45. Canellas AR, Gols AR, Izquierdo JR, et al. Idiopathic inflammatory-demyelinating diseases of the central nervous system. Neuroradiology 2007;49(5): 393–409.
46. Given CA 2nd, Stevens BS, Lee C. The MRI appearance of tumefactive demyelinating lesions. AJR Am J Roentgenol 2004;182(1):195–9.
47. Cha S, Pierce S, Knopp EA, et al. Dynamic contrast-enhanced T2*-weighted MR imaging of tumefactive demyelinating lesions. AJNR Am J Neuroradiol 2001;22(6):1109–16.
48. Masdeu JC, Moreira J, Trasi S, et al. The open ring. A new imaging sign in demyelinating disease. J Neuroimaging 1996;6(2):104–7.
49. Tien RD, Felsberg GJ, Osumi AK. Herpesvirus infections of the CNS: MR findings. AJR Am J Roentgenol 1993;161(1):167–76.
50. Baskin HJ, Hedlund G. Neuroimaging of herpesvirus infections in children. Pediatr Radiol 2007;37(10): 949–63.
51. Heiner L, Demaerel P. Diffusion-weighted MR imaging findings in a patient with herpes simplex encephalitis. Eur J Radiol 2003;45(3):195–8.
52. Kuker W, Nagele T, Schmidt F, et al. Diffusion-weighted MRI in herpes simplex encephalitis: a report of three cases. Neuroradiology 2004;46(2):122–5.
53. Duckworth JL, Hawley JS, Riedy G, et al. Magnetic resonance restricted diffusion resolution correlates with clinical improvement and response to treatment in herpes simplex encephalitis. Neurocrit Care 2005; 3(3):251–3.
54. Sener RN. Herpes simplex encephalitis: diffusion MR imaging findings. Comput Med Imaging Graph 2001;25(5):391–7.
55. Takasu A, Taneda M, Otuki H, et al. Gd-DTPA-enhanced MR imaging of cryptococcal meningoencephalitis. Neuroradiology 1991;33(5):443–6.
56. Tschampa HJ, Zerr I, Urbach H. Radiological assessment of Creutzfeldt-Jakob disease. Eur Radiol 2007;17(5):1200–11.
57. Zerr I, Pocchiari M, Collins S, et al. Analysis of EEG and CSF 14-3-3 proteins as aids to the diagnosis of Creutzfeldt-Jakob disease. Neurology 2000;55(6): 811–5.
58. Will RG, Ironside JW, Zeidler M, et al. A new variant of Creutzfeldt-Jakob disease in the UK. Lancet 1996;347(9006):921–5.
59. Hildenbrand P, Craven DE, Jones R, et al. Lyme neuroborreliosis: manifestations of a rapidly emerging zoonosis. AJNR Am J Neuroradiol 2009;30(6): 1079–87.
60. Lyme disease—United States, 2003–2005. MMWR Morb Mortal Wkly Rep 2007;56(23):573–6.
61. Agarwal R, Sze G. Neuro-lyme disease: MR imaging findings. Radiology 2009;253(1):167–73.
62. Rafto SE, Milton WJ, Galetta SL, et al. Biopsy-confirmed CNS Lyme disease: MR appearance at 1.5 T. AJNR Am J Neuroradiol 1990;11(3):482–4.
63. Fernandez RE, Rothberg M, Ferencz G, et al. Lyme disease of the CNS: MR imaging findings in 14 cases. AJNR Am J Neuroradiol 1990;11(3):479–81.
64. Archibald SL, Masliah E, Fennema-Notestine C, et al. Correlation of in vivo neuroimaging abnormalities with postmortem human immunodeficiency virus encephalitis and dendritic loss. Arch Neurol 2004;61 (3):369–76.
65. Thurnher MM, Schindler EG, Thurnher SA, et al. Highly active antiretroviral therapy for patients with AIDS dementia complex: effect on MR imaging findings and clinical course. AJNR Am J Neuroradiol 2000;21(4):670–8.
66. Sarrazin JL, Soulie D, Derosier C, et al. [MRI aspects of progressive multifocal leukoencephalopathy]. J Neuroradiol 1995;22(3):172–9 [in French].
67. Kuker W, Mader I, Nagele T, et al. Progressive multifocal leukoencephalopathy: value of diffusion-weighted and contrast-enhanced magnetic resonance imaging for diagnosis and treatment control. Eur J Neurol 2006;13(8):819–26.
68. Mader I, Herrlinger U, Klose U, et al. Progressive multifocal leukoencephalopathy: analysis of lesion development with diffusion-weighted MRI. Neuroradiology 2003;45(10):717–21.
69. Ohta K, Obara K, Sakauchi M, et al. Lesion extension detected by diffusion-weighted magnetic resonance imaging in progressive multifocal leukoencephalopathy. J Neurol 2001;248(9):809–11.
70. Tan K, Roda R, Ostrow L, et al. PML-IRIS in patients with HIV infection: clinical manifestations and treatment with steroids. Neurology 2009;72(17): 1458–64.
71. Kastrup O, Wanke I, Maschke M. Neuroimaging of infections of the central nervous system. Semin Neurol 2008;28(4):511–22.